

---

Thesis Submitted in Partial Fulfillment of the Requirements for the  
Degree of Master in Science in Textile Engineering  
The Swedish School of Textiles  
2014-05-19

Report no:  
2014.14.02

---

# Textile Sensor Using Piezoelectric Fibers for Measuring Dynamic Compression in a Bowel Stent

- An Experimental Study -

Author: Anna Vahlberg



THE SWEDISH SCHOOL  
OF TEXTILES  
UNIVERSITY OF BORÅS

**Description:** Thesis submitted for the degree of Master in Science in Textile Engineering

**Title:** Textile Sensor Using Piezoelectric Fibers for Measuring Dynamic Compression in a Bowel Stent

**Author:** Anna Vahlberg

**Supervisor:** Anja Lund

**Cooperation partners:** Swedish School of Textile and the Department of Surgery at Södra Älvsborgs Sjukhus

**Examiner:** Vincent Nierstrasz

The Swedish School of Textiles  
Report No. 2014.14.02

## **Abstract**

In this experimental study the in-lined poled piezoelectric poly(vinylidene fluoride)(PVDF) bicomponent fiber was investigated the suitability in applications within the area of textile sensors when used in a bowel stent. Today there are only piezoelectric films made of PVDF available. Compared to a film, a fiber increases the amounts of application abilities.

In this study a plain weave, resembling a coordinate system was made of the piezoelectric PVDF fiber and tested on top of two different beds; one hard and one elastic made of foam. The structure was then developed into two structures; one integrated in the stents structure with a plain weave pattern and one secondary structure as a plain weave placed onto the stent. Two test methods were developed in order to resemble the bowel movements to test the two piezoelectric PVDF fiber based structures. A reliability test in a reometer was made of the fiber, giving high differences in mean values. An in vivo test was conducted in a pig where the stent was placed in the orifice of the stomach.

Both structures shown response when both developed methods was used. Due to large irregularities within the piezoelectric PVDF fiber the evaluation between the two structures was not possible. The most favorable structure was the secondary structure due to the larger continuous process ability and application areas. It was also seen that the reliability of the piezoelectric PVDF fiber is low, giving a non-reliable sensor.

**Key words:** Piezoelectricity, advanced textile structure, textile sensor, piezoelectric poly(vinylidene fluoride), (PVDF), textile medical device, self-sensing stent.

## **Popular Abstract**

Piezoelectricity is a phenomenon when a piezoelectric material is pressed which generates a voltage output. There are several textile polymers where the phenomenon can be created, one of those is poly(vinylidene fluoride) (PVDF). Recent research at Swerea IVF and the Swedish School of Textiles have found that it is possible to make a piezoelectric fiber of PVDF. In this study it was investigated whether or not the fiber is suitable as a textile sensor measuring muscle movements placed in a stent used for the bowel.

Two structures were investigated in this study; one where the piezoelectric PVDF fiber was integrated in the structure of the stent and the other as a secondary structure sewn onto the structure of the stent. Two test methods were developed to resemble bowel movements. An animal test on a pig was done in order to test when the stent was subjected to real muscle movements.

It was shown that it is possible to use both structures as textile sensors to measure muscle movements in a bowel. The most favorable structure when considering the versatility was the secondary structure.

## Table of content

1. Introduction .....	1
1.1 Background description .....	1
1.2 Aim.....	2
1.2.1 Research questions .....	2
1.3 Delimitations .....	2
2. Theory.....	3
2.1 Smart textiles.....	3
2.1.2. Textile sensors.....	3
2.2 Piezoelectricity .....	4
2.3 Piezoelectric polymers .....	5
2.3.1 Poly (vinylidene fluoride) PVDF .....	5
2.4 Poling.....	6
2.5 Inner and outer electrode .....	6
2.6 The stent and the human body.....	7
2.6.1 Stents .....	7
2.6.2 Basic anatomy and placing of the stent .....	8
2.7 EndoFLIP – measuring the compressions within a bowel stent.....	9
2.8 Patents and other measuring systems for the bowel.....	9
2.8.1 Measuring system for the bowel .....	9
2.8.2 Stent with a piezoelectric element .....	10
2.8.3 Other patents with sensing stents.....	10
3. Materials used in this study .....	11
3.1 The piezoelectric yarn – a bicomponent fiber .....	11
3.3 Conductive material.....	11
3.3.1 Silver paint.....	11
3.3.2 Copper tape.....	11
3.3.3 Copper thread.....	11
3.3.4 Coating.....	11
3.4 Attachment materials .....	11
3.4.1 Thread.....	12
3.4.2 Glue .....	12
3.5 Stent.....	12
3.6 Secondary structure .....	12

4 Method.....	13
4.1 Yarn making for samples.....	13
4.1.1 Pre-shrinking and pre-shrinkage test .....	13
4.1.2 Coating.....	13
4.1.3 Preparation of connection to the inner electrode.....	13
4.1.4 Pre-testing of piezoelectricity.....	13
4.2 Replicability test.....	14
4.2.1 Testing in low pH.....	14
4.3 Textile structures.....	15
4.3.1 First sample.....	15
4.3.2 Integrated textile structure.....	16
4.3.3 Secondary textile structure .....	17
4.4 Methods for simulating bowel movements.....	17
4.4.1 Ring compression method .....	18
4.4.2 Ring movement method .....	19
4.5 Testing of the stent.....	20
4.5.1 Test with ring compression method.....	21
4.5.2 Test with ring movement method.....	22
4.6 Testing after poled in direct contact.....	22
4.7 In vivo .....	22
5. Result.....	24
5.1 Pre-shrinking .....	24
5.2 Replicability test .....	24
5.1.2 Testing in low pH.....	24
5.3 Sample 0.....	25
5.4 Ring compression testing.....	25
5.4.1 Sample 1.....	26
5.4.2 Sample 2.....	27
5.4.3 Double sided test.....	28
5.5 Ring movement testing .....	29
5.4.1 Sample 1.....	29
5.4.2 Sample 2.....	30
5.4.3 Double sided test.....	30
5.6 Testing after poled in direct contact.....	31

5.7 In vivo testing.....	32
6. Discussion.....	33
6.1 Shrinkage test .....	33
6.2 Textile structures and sample selection .....	33
6.2.1 Sample 0.....	34
6.2.2 Sample 1 .....	34
6.2.3 Sample 2.....	34
6.3 Material selection.....	34
6.4 Construction of testing methods.....	35
6.5 Applicability of testing methods to different stents.....	36
6.6 Replicability test .....	36
6.7 Poling in direct contact.....	37
6.8 In vivo testing.....	37
6.9 Evaluation of the developed test methods after the in vivo testing.....	37
6.10 Application in the bowel.....	38
7. Conclusion .....	40
8. Further Research .....	40
9. Acknowledgement.....	41
10. References.....	42
Appendix A – Ring compression method .....	i
Appendix B – Ring movement method .....	ii
Appendix C – Sample 0.....	ii
Appendix D – Curves ring compression method .....	vi
Appendix E – Curves ring movement method .....	xii

## 1. Introduction

Textile based sensors are considered to be a smart textile. The definition of a smart textile is: a material or structure which has the ability to sense and react to surrounding conditions and stimuli. One example of a stimulus is mechanical e.g. dynamic compression. The major reason for why the development occurred is the flexibility and drapability of a textile. These abilities increases e.g. comfort in a worn item. (Schwarz, A. et al.,2010)

### 1.1 Background description

A stent is a device used for keeping the patency of a hollow organ in order to secure liquid flow. Today the use of stents has increased from the initial application in the throat to a number of different areas. The range goes from usage in blood vessels to the bowel<sup>1</sup> for keeping the patency and enabling liquid flow, additionally covering holes and gaps. Usually they are preferred to use instead of major surgery and are considered to be very helpful. Though, the stent itself can cause problems, such as ingrowth. (O'Brien, C, & Sparkman, 1997)

A piezoelectric material such as poly(vinylidene fluoride) (PVDF) has the ability to generate voltage when a mechanical stress is subjected. (Lund. A., et. al. 2012) Today, the piezoelectric PVDF can be found in energy harvesting devices. There are also several applications within the medical area e.g. for measuring heart beats while integrated in a stent for blood vessels. (Ward K., et al., 2005) The PVDF is a commercially available polymer and can be found in many application areas such as resonators, speakers, measuring pressure, vibration and acceleration. (Fulmer, 1998)

There is a need to measure the bowel movements without extra forces applied than of the stent. During surgery the surgeons have seen that the bowel movements actually increases when put under pressure from forceps. It is crucial to understand why and how the bowel moves since stents used in the orifice of the stomach or in the bowel starts moving away from the intended area after only one week. By increasing the knowledge of the bowel movements the design of the stent can be improved. (Bergström & Park, 2014)

---

<sup>1</sup> Bowel describes the whole digestive tract from the mouth to the anus in animals. When used describing human anatomy the bowel describes the digestive tract after the stomach to the anus. (Nationalencyklopedin, 2014)

## 1.2 Aim

The aim with this study is to investigate whether a piezoelectric fiber could be used as a textile sensor, sensing dynamic compression when integrated in a stent used for the bowel.

### 1.2.1 Research questions

The main research questions for this master thesis are addressed as follows:

1. Can a piezoelectric PVDF fiber be used measuring dynamic compression radially in a stent placed in a bowel?
  - a. Can a matrix of piezoelectric PVDF yarns be used to place to locate the point of pressure in a textile structure and illustrate the pressure distribution in real-time?
2. Which textile production method is suitable to integrate the piezoelectric fiber be integrated in a textile structure such as a stent?
  - a. Is it beneficial to integrate the piezoelectric fiber directly into the structure of the stent in order to measure bowel movements?
  - b. Is it beneficial to integrate the piezoelectric fiber via a secondary structure used on the surface of the stent in order to measure bowel movements?

## 1.3 Delimitations

The master thesis is limited to use a piezoelectric material made of a PVDF bicomponent fiber with a core of carbon black (CB) and high density polyethylene (HDPE). The incorporation of the piezoelectric fiber is done in stents made for the bowel. During the manufacturing the fiber was in-lined poled at Swerea IVF, a continuous textile process. The primary aim is to use a continuous textile processed fiber. Materials used must withstand a temperature of 120° C due to the conditions to cure the outer electrode. A conductive silicone coating with CB was used as an outer electrode in this study, however when used in living bowel this may be excluded due to the body liquids are conductive. The piezoelectric characterization was limited to measuring the voltage output during compression using a four channel PicoScope<sup>2</sup> at the Swedish School of Textile.

---

<sup>2</sup> A PC Oscilloscope where all data is transferred directly from the oscilloscope to a computer and used for recording output voltage. (PicoTech, 2014)

## 2. Theory

Within this chapter important subjects and aspects of the project are introduced. A brief introduction of what a smart textile is as well as what piezoelectricity is. A simple description of the stent and the anatomy of the bowel are also included.

### 2.1 Smart textiles

Today there is a lot of research conducted worldwide within the area of smart textiles. Six functions have been defined which a smart textile system can have; sensing, actuating, powering, communication, data processing and interconnecting. Though the smart functions may not be actual textile, but electronics incorporated within the textile. The system is still considered to be a smart textile. The precondition is the system e.g. a garment should be flexible, high in comfort when worn and durable to ordinary textile maintenance such as washing. (Schwarz, A. et al.,2010)

The smart textile systems are divided after their abilities in three major groups:

- Passive smart textiles
- Active smart textiles
- Very smart textiles

The function of a *passive smart textile* is the sensing function and is the most simplest. An *active smart textile* has the function of sensing stimulus but can also react upon it. The *very smart textiles* have the ability to sense, react and the gift to adapt to the new circumstances. There are a number of different stimuli smart textiles can react on e.g. chemicals, pressure, temperature and pH. (Schwarz, A. et al.,2010)

#### 2.1.2. Textile sensors

The definition of a sensor is a *device which provides information* and the information is usually in the form of electrical signal. A smart textile in the form of textile sensor has the sensing function, thus it can sense changes in the environment. Usually when the application is within the smart textile area, the sensors used are piezo-resistive and pressure sensors. A large part of the smart textile development is actually the development of textile sensors. The majority of the sensors have their application within the medical field. (Schwarz, A. et al.,2010) Research has been done where textile based sensors was used in order to monitor heart rate. (Gupta, 2010) (Osman R. M. A., et al., 2011)

Sensors are usually divided into two major groups for classification reasons; active and passive sensors. A passive sensor, as the name suggests require an external power source in order to function and to convert the input into a useable response. Whereas an active sensor does not need an external power source in order to convert the input energy. Thus within the smart textiles area, a passive sensor is usually made out of conductive fibers and an active sensor can be based on the piezoelectric effect. (Carpi & De Rossi, 2005) There is a patent where the

function is described to be measurement of the heart rate and energy harvesting within a stent placed in the coronary blood vessels using piezoelectric PVDF. (Ward K., et al., 2005) The patent is described further in section 2.8.2.

### 2.1.2.1 Reliability of a sensor

When a sensor is evaluated, whether or not it is suitable for the application in aspect of e.g. detection area or optimal arrangement of components, a common evaluation is to investigate the reliability of the sensor. The properties concerning the sensors detection area is set before the evaluation is taken part. Since detection area is one of the major factors when determine if a sensor is reliable or not. A “black spot” within the detection area is not suitable, giving the sensor a low reliability. Additionally, it is crucial the “black spots” are not due to irregularities within the sensor component material. Thus the material itself in a sensor needs to be reliable in order for the sensor to be reliable. (Noguchi, 1997)

## 2.2 Piezoelectricity

Piezoelectricity can be defined as changes in polarization proportional to the applied strain. (Tichý J. et al., 2010) Whether or not a material can be piezoelectric is dependent on the crystalline unit structure. If the crystalline unit has an atomic structures which is arranged non-symmetrical, the crystals will act as dipoles. (Lando & Doll, 1968) The piezoelectric properties can be found in various number of materials such as; ceramics, polymers and silk. (Harrison & Ounaies, 2014)

When a material is piezoelectric and a mechanical stress is applied, the dielectric displacement will increase as a response to the applied stress. The phenomenon is called the direct effect. It is also possible to direct it the phenomena the other way around, giving a mechanical deformation is induced by an electrical charge. When the phenomenon is induced by an electrical charge the effect is called the converse effect. (Harrison & Ounaies, 2014) When producing pressure and compression sensitive sensors the use of the direct effect is ideal. (Ashruf, 2002) The compression caused by pressure, which gives an output is shown in figure 1.

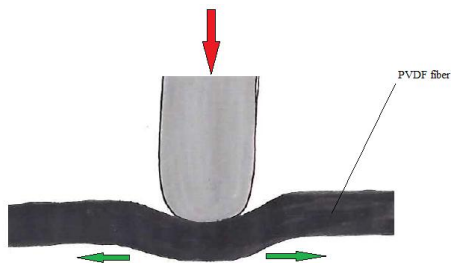


Figure 1 A single PVDF fiber when undergoing compression from an object (red arrow) giving compression in the interface between the fiber and the object causing strain in the bottom of the fiber (green arrows).

In order to characterize the piezoelectric properties of a material two piezoelectric coefficients can be used. (Lund & Hagström, 2010) The first is the voltage constant  $g$  and the other is the strain constant  $d$ . The voltage constant relates electrical charge produced due to an applied mechanical stress and the strain constant relates the mechanical strain produced when an electrical charge is applied to the material. (Das-Gupta & Doughty, 1978)

Piezoelectric materials are more suited for measuring dynamic strain and compression. However it is not suitable to use them in sensors measuring static load due to a leakage of current. At first the piezoelectric material will have an output due to the dynamic strain change and if the load is kept constant the output will decrease back to zero. (Ashruf, 2002) If there is a need to measure both static load and dynamic compression the piezoelectric material must be combined with a material that has the ability to measure static load.

## 2.3 Piezoelectric polymers

There are several different textile fibers that can be man-made into piezoelectric materials, such as PVDF, polypropylene (PP), polyethylene terephthalate (PET) and polyamides with odd numbers (e.g. PA5). (Qaiss A. et al., 2012) (Liu, Z. H. et al., 2013) (Murata Y. et al., 1998) Polymers are more suitable to make sensors than e.g. ceramics. The polymers have a higher piezoelectric voltage than the ceramics. Due to the ability for all the named polymers to be processed as a textile fiber, the sensors made by a polymer can be more flexible than one made of brittle ceramics. But there are several other favorable attributes polymers have compared to ceramics; low density, low dielectric constant and low elastic stiffness. Combined, these properties gives the piezoelectric polymers a property preferred when producing a sensor; a high voltage sensitivity. (Harrison & Ounaies, 2014)

### 2.3.1 Poly (vinylidene fluoride) PVDF

The polymer PVDF is as the name suggests several monomers which are connected into a longer chain: a polymer chain. Due to the differences in charges, each monomer has an inherent dipole moment. (Sirohi & Chopra, 2000) As seen in figure 2 the hydrogen (H) atom is slightly charged positive and the fluorine (F) atom is negatively charged when the carbon (C) atom is considered. The PVDF has the ability to crystallize in four different phases. The most favorable phase to achieve the highest piezoelectric effect it is the  $\beta$ - phase the Form I. The  $\beta$ - phase has a high polarity compared to the other phases which can be seen in figure 2. The  $\beta$ - phase is in trans conformation. PVDF usually crystallize in the form of the  $\alpha$ -phase the so called Form II. (Lando & Doll, 1968) The most favorable phase energetically is the  $\alpha$ -phase. Due to the configuration of the monomers, a conformation of trans and gauche the  $\alpha$ -phase is non-polar. (Hasegawa R. et al., 1972)

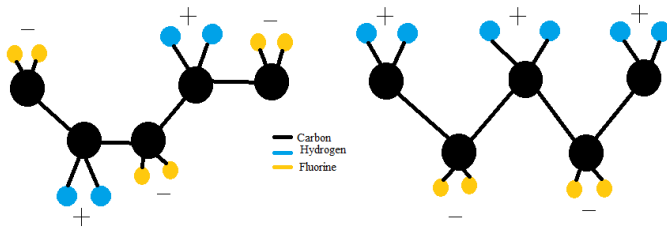


Figure 2 Configuration of the two PVDF phases;  $\alpha$ -phase (left) and  $\beta$ - phase (right). Note how the atoms of different polarity are placed in the two forms and uniformity of the placement in the  $\beta$ - phase.

The conformation of the  $\alpha$ -phase has the possibility to convert to the  $\beta$ - phase. The conversion is possible by applying mechanical stress at a certain temperature. (Matsushige & Takemura, 1983) After the mechanical stretch, all the  $\beta$ - phase crystallites are randomly oriented within the material. (Dargaville, o.a., 2005) To achieve the piezoelectric property a poling process is necessary. Not everything is yet known of what is happening in the poling process, except that the crystals in the polymer are affected by the electrical field and creates a net polarization. Due to the net polarization all the crystals align. The alignment of the crystals changes when a mechanical stress is applied to the material. The change in alignment causes a energy change at the surface. To be able to register these energy changes two electrodes needs to be connected on each side of the material. (Lund, A. et al., 2012)

## 2.4 Poling

The principle of poling a material can be described as; a material is exposed to an electrical field either in a contact or non contact mode. When a material is poled in contact mode two electrodes are connected to both sides of the material. The electrodes are connected to a high voltage supply. On the other hand when in non contact mode the material is placed between a high potential electrode and a grounded counterpart. The non contact mode goes under the name corona poling. Recent studies have shown that the corona poling does not have as high effect on the net polarization as the direct poling has. (Nilsson, E. et al., 2013)

## 2.5 Inner and outer electrode

In recent studies, the electrode can be incorporated in the fiber structure while being melt spun as a bicomponent fiber. The electrode would then be an inner electrode. The most favorable placement of the electrode is along and placed in the core of the fiber. For this study the conductive material in the inner electrode is CB. In order to have as much output as possible the outer electrode needs to cover a large area. (Lund, A. et al., 2012)

In order to be able to collect the generated charges from the PVDF sheath of the bicomponent fiber an outer electrode has to be applied. (Lund, A. et al., 2012) There has been shown in recent studies that it is possible to use different conductive materials e.g. CB in combination with HDPE and conductive silicone rubber (Lund, A. et al., 2012) (Nilsson, E. et al., 2013). Though, it is not always positive to use a non-metallic outer electrode. Due to the higher resistance in the

non-metallic materials the piezoelectric output voltage will decrease. (Nilsson, E. et al., 2013)

## 2.6 The stent and the human body

In this section the application of the stent is briefly described as well as the basic anatomy and properties of the stomach and bowel.

### 2.6.1 Stents

The word stent and the meaning of the stent started appearing in print and used as a surgical vocabulary in the beginning of the 1970s. (Bloom, D. A. et al., 1999) A stent is a cylindrical device used to ensure the patency of an anastomosis<sup>3</sup>, often to allow drainage of the specific area. (O'Brien, C, & Sparkman, 1997) It was in the beginning of the 1990s when the uses of stents in the gastrointestinal tract first was described. (Kang, 2010) A vast number of the development of the stents today, is in the area of cardiovascular diseases. But there is still development of stents for the bowel. However, the research is very inspired by the development of the stents for blood vessels. The major mechanical properties desired for the stent is a durable wall and a high radial force. These properties are altered when the application and the size of the stent is changed. Stents with the property of a high expandability have a tendency of a higher degree of a restoring force when bent. Unfortunately, if these are used somewhere which is inappropriate, the stent can actually cause ulceration or perforation. (O'Brien, C, & Sparkman, 1997)

There are two major groups of stents used today; covered and uncovered. The covered ones are used when the stent is inserted where it must keep the patency or reduce obstructions but also to cover any openings e.g. ulcers<sup>4</sup>. The covered stent has the theoretical advantage to reduce the tumour ingrowth. Though, due to being covered the friction is reduced causing an increase in migration compared to a non covered stent. The second, the uncovered has the advantage of less migration than the covered stent, but instead has higher possibility of ingrowth. The higher risk of ingrowth in an uncovered stent is due to the application, often in the bowel when a tumour reduces the patency of the bowel. The area where the stent is placed gives large compression forces causing the tissue into the structure of the stent. The tumour also holds the stent in place in a higher degree than the covered stent. (Maudgil, D. D. et al., 2001)

A popular type of stents, so called self-expanding metallic stents (SEMS) is often used while treating acute colonic obstruction and can be seen in figure 3. They were first described by Dohmoto in 1994. The SEMS have been used in two major areas; firstly, in bowel obstructions for patients with metastatic cancer or patient to sick for a major surgery. The second; used as a “bridge to surgery”

---

<sup>3</sup> A natural or manmade, by surgery connection between aperture means e.g. between different parts of the bowel or between blood vessels. (Nationalencyklopedin, 2014)

<sup>4</sup> A so called bleeding ulcer is when gastric juice leaks out in the abdominal and can cause major infections and pains. (Thachuk, 2008)

meaning having more time to optimize the health of the patient before a major surgery and reducing the need of a stoma. (Mackay, C. D. et al., 2011)

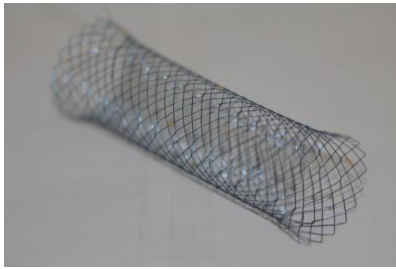


**Figure 3 A SEMS-stent displayed.**

There are several studies in order to develop several new manufacturing processes when producing a stent and what type is used depends on; what application area, chosen material and desired mechanical properties. E.g. 3D printing system for making a tracheal stent (Melgoza, E. L. et al., 2014) and fiber laser cutting (Meng, 2009) Due to the many possibilities to produce a stent, the difficulty of analyzing what textile process the stent was made of by examine the stent ocularly is high.

### **2.6.2 Basic anatomy and placing of the stent**

The stomach can be considered as a container for food and a part of the digestive system. In order to digest the food the stomach produces hydrochloric acid<sup>5</sup> and secretes the enzyme pepsin. Due to the low pH, which is often in the range of 1-1.5, most of the bacteria carried by the nourishment die. The orifice of the stomach feeds by large muscle contractions the partly digested food into the duodenum, a part of the small intestine, where all nutrients are absorbed by the walls. The remains are pushed forward by the muscles in the bowel wall when contracting causing undulation. The motion is increased by the fact that the digested food is mainly liquids. The remains are mainly a mixture of: sugars, fats, amino acids, vitamins, salts and tracers. (Ellis & Mahadevan, 2013)

There are several places in the bowel area the stent could be placed, since the bowel is approximately 8 meters long. (Nationalencyklopedin, 2014) Since the digestive system is versatile in the movements, especially when comparing the orifice of the stomach and the bowel. Due to the versatility the stent may need different properties in different applications e.g. a stent placed in the orifice of the stomach may need different mechanical properties than a stent placed in the duodenum. Different placement can be seen in figure 4.

---

<sup>5</sup> Hydrochloric acid has the main function of protect the body from digested microorganisms. (Nationalencyklopedin, 2014) It is the hydrochloric acid which gives the low pH in the stomach causing a hostile environment for the microorganism. Hydrochloric acid is basically when in liquid form positive and negative ions. (Atkins & Jones, 2010) The acid is conductive due to its different charges, since a current is defined as a movement or flow of electrically charged particles. (Serwey & Jewett, 2013) Other bodily functions such as nerv signal are transported due to this phenomenon. (Jezernik & Grill, 2001)

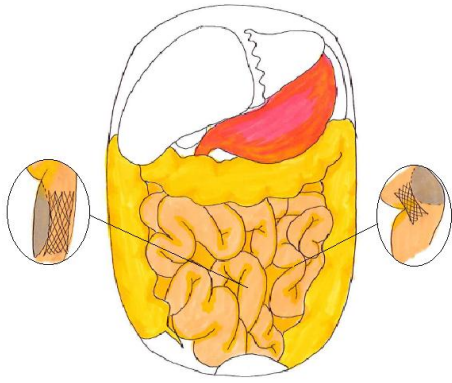


**Figure 4** An overview of the placement of the organs are in the human body where the described organs are colored. The figure also shows examples of different stent placement in the abdomen. The grey areas represent in this example, cancer tumors which cause the blockage in the bowel. The placement to the left represent when the placement of the stent is straight and to the right when the placement is where the intestine is convoluted which could enhance displacement.

## 2.7 EndoFLIP – measuring the compressions within a bowel stent

There are today few ways of measuring bowel movements. One of the most used methods is EndoFLIP (Endolumenal Functional Lumen Imaging Probe) measuring system. It is used to measure hollow organs and sphincteric<sup>6</sup> regions within the gastrointestinal<sup>7</sup> tract. The technique inserts a balloon catheter where the measured area is. A conductive solution is injected into the balloon catheter. Due to the liquid applied, from the inside, a force is applied to the measured area in the bowel. Within the balloon an array of electrodes are situated measuring voltages. With the help of the measured voltage the diameter is estimated and with the help of a software program projects in 3D the differences in diameter. (Crospon Inc, 2014)

Due to the applied pressure from within the EndoFLIP measuring system, the actual measurement is not measuring the implication the stent has done to the bowel movements but also what the EndoFLIP induces. Due to the increase of the bowel movement caused by the measuring method, the EndoFLIP is not ideal to use when measuring force impact and dynamic forces caused by the stent. (Bergström & Park, 2014)

## 2.8 Patents and other measuring systems for the bowel

Measuring systems used previously are described as well as relevant and recent patents within the area are described.

### 2.8.1 Measuring system for the bowel

During a study where the variations in movements from the esophagus to the colon were investigated a measuring system was used. The recording system was

<sup>6</sup> A sphincter is a muscle which has the shape of a ring. The function is to close an orifice or passage e.g. the orifice of the stomach. (Nationalencyklopedin, 2014)

<sup>7</sup> A medical term to describe something that belongs to the digestive tract. (Nationalencyklopedin, 2014)

built of four polyvinyl tubes where 12 sideholes were cut. Inside each tube three lumens were located, additionally with 12 sensors. The total length of the tube was 185 cm. The individual study lasted for two days, where the objects were fasting the first day and having a liquid meal the second day. The data recorder were; velocity of propagation (cm/min), maximum frequency of contractions (No./min) and the duration (min). The results varied largely depending on the measurement area. The frequency range was from 6.1 to 11.7 No/min, where the highest was found closer to the stomach and the lowest in the colon area. (Kellow, J. E. et al., 1986)

### **2.8.2 Stent with a piezoelectric element**

There exists one patent describe where a piezoelectric PVDF fiber is incorporated in a stent as an active part of a sensor called “Self-sensing Stents” CA 2633419 A1. The patent describes a medically implantable stent where the content is of at least one piezoelectric material. There are several new properties described for the stent which is not found in stents in the commercial market; anticoagulant delivery or any other therapeutic effect, self powering as well as sending an electrical signal to device outside of the body giving the physician the possibility to estimate the condition of the surrounding tissue. The described application areas for the stent: placement in the heart e.g. the coronary artery, vascular, airways, gastrointestinal, urologic and for drug-eluting. The piezoelectric element gives the stent the possibility to remotely change the amount of drug-release, harvesting energy which would be used for drive various actuators which can be activated with an external electrical signal. Due to the piezoelectric element a battery is excluded. The piezoelectric element gives and voltage output from the pulsatile flow through the stent of e.g. blood flow, airway flow, urine flow and bile flow. (Ward, Ounaies, & Vetrovec, 2005)

### **2.8.3 Other patents with sensing stents**

There are numerous different patents concerning sensing stents, two are briefly described in this section due to the large similarities between the sensing systems.

Firstly the “Stent flow Sensor” where the placement for the stent is in a blood vessel, where a Micro-Mechanical System (MEMS) ultrasound generator is used for determining patency of the blood vessel and flow rate through. Also any pressure drop is measured from the one end to the other. A transmitter is used to provide the signals to an externally placed receiver. (Hoffer, 2009) Secondly, the pressure-sensing stent is for vascular measurement, while placed in the human body. A flow parameter sensor is used to measure rate or flow through the stent and transmits the signal to a receiver placed outside of the body. (Govari & Fenster, 1997)

### **3. Materials used in this study**

In the following sections the specific materials used for this project are described more detailed. The dimensions were measured with a Masuer caliper.

#### **3.1 The piezoelectric yarn – a bicomponent fiber**

The bicomponent PVDF fiber as a yarn of 950 dtex was used in the warp and weft of the grid used integrated in the stent and as the secondary structure on top of the stent. The yarn was made of 24 filaments each 39.6 dtex. The material used for the sheat in the bicomponent fiber was PVDF homopolymer, (Solef 1006). The core material is used as an inner electrode due to its electrical conductivity. The core material is a mixture of HDPE (ASPUN 6835A) and 30 % carbon black (Ensaco 260) which was used to create the conductivity. While melt-spinning the PVDF fiber was drawn with a solid state draw (SSDR) of 2.3. During the spinning the bicomponent fiber was in-lined poled with the voltage of -9 kV. In order to achieve the in-line poling one of the last stretching wheels was removed in favor of the in-line poling equipment. The sample was made 2013-12-11 at Swerea IVF in Mölndal. The technical data was provided by Swerea IVF.

#### **3.3 Conductive material**

The materials used, due to its conductivity is described in the following sections.

##### **3.3.1 Silver paint**

The conductive material used for connecting the inner electrode was a silver paint called “Agar Silver Paint” from Agar Scientific Ltd. containing silver particles.

##### **3.3.2 Copper tape**

A conductive copper tape from 3M was used to connect the silver paint and additionally the inner electrode. The conductive tape gives a higher surface for the probes to be attached upon.

##### **3.3.3 Copper thread**

A conductive thread made of copper was used to extend the outer electrode while testing. The thread was a monofilament from Leoni with a diameter of 0.1 mm.

##### **3.3.4 Coating**

One material was used in this study as an outer electrode. A coating was chosen due to its ease in applying evenly compared to twist the PVDF with a conductive yarn. A thin layer of Elastosil® LR 3162 A/B from Wacker Chemie AG is applied to the surface of yarn. The coating is an electrically conductive two component silicone rubber. The vulcanization of the rubber is done by mixing the A- and B-component and with a relative short curing time with heat. The estimated conductivity given by the supplier is 0.09 S/cm.

#### **3.4 Attachment materials**

The materials used in order to fasten the piezoelectric PVDF fiber are described in following two sections.

### 3.4.1 Thread

The material used to fasten the piezoelectric fiber to the carrier and the stent was a thread used in overlock machines. The thread was from the company Ackermann-Göggingen AG and called “Synton” with 160/2 dtex and made of polyester.

### 3.4.2 Glue

In order to fasten the piezoelectric fiber in the stent structure, a glue was used from Loctite called Superglue Precision was used.

### 3.5 Stent

The stents used in this study kindly supplied by Södra Älvsborgs Sjukhus were manufactured by M.I. Tech (Korea) a “Hanarostent” made for use in the bowel. It is of a SEMS type, the dimensions are given in figure 5. The stent has larger flare ends for an anti-migration effect, flexible structure and radiopaque<sup>8</sup> markers.

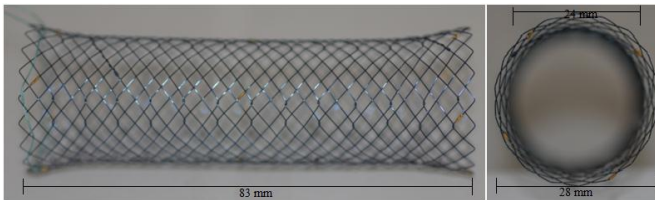


Figure 5 A display of the stent used in this study. All the dimensions are given while measuring in an uncompressed state which varies if any force is applied.

### 3.6 Secondary structure

The material used for the secondary structure is a mosquito net found in many conventional stores. The one used in this study has the weave construction of a plain weave see figure 6. The warp and weft are made of polyester filament yarns. The whole structure is coated after weaving with polyvinylchloride (PVC) in a grey color, giving a stable no shearing structure but still a drapable textile.

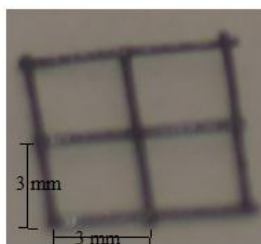


Figure 6 The plain weave mosquito net displayed showing that the plain weave has a quadratic shape.

<sup>8</sup> Visible while taking x-ray photographs.

## 4 Method

This chapter presents the preparation of the used materials, how the different testing structures were made, describing developed methods and how the characterization was conducted.

### 4.1 Yarn making for samples

The different steps in preparing the yarn are described in detail below.

#### 4.1.1 Pre-shrinking and pre-shrinkage test

All bicomponent PVDF yarns were pre-shrunk before use. The pre-shrinking was made by placing the yarn on paper and placed in an oven with temperature 120° C for 1 hour. After heating, the samples were left reduce the temperature to room temperature before other use or process.

Due to the observation, while handling the fiber in high temperatures, the fiber shrunk, a “pre-shrinkage test” was conducted. 10 meters of the bicomponent PVDF was taken and carefully cut into 10 pieces of 1 meter. The pieces were heated in an oven at temperature 120° C for 1 hour. After heating, all fiber pieces were left to reduce the temperature to room temperature. All samples were carefully measured post heating and compared to initial length.

#### 4.1.2 Coating

All samples were prepared with coating Elastosil® LR 3162 A/B. The two component silicone rubber coating was mixed in ration of 1:1, according to the manufacturer’s instructions. The coating was carefully applied to the bicomponent PVDF fiber which was placed on greaseproof paper, with a spatula. The spatula was used to cover and align the filaments. The samples were moved onto a second greaseproof paper. The coated fibers were cured in an oven at temperature 120° C for 1 hour. All samples were reduced to room temperature before other use.

#### 4.1.3 Preparation of connection to the inner electrode

To be able to connect the core of the fiber, the inner electrode, a paste was needed to be applied. A scalpel was used to cut the fiber. The scalpel has a lower degree of shearing to the fiber ends than a scissor when cutting. The paste “Agar Silver Paint” was smeared at the end of the fiber and approximately one centimeter further along the fiber. A piece copper tape was applied on top of the silver paint, enabling a steady connection to the probe. The other fiber ends was sealed off with Superglue Precision in order to avoid short cuts in the circuit.

#### 4.1.4 Pre-testing of piezoelectricity

Every fiber was characterized with respect to its piezoelectric activity before any application to make sure the production of each sample was successfully made. The inner and outer electrode was connected to a PicoScope 5000 Series. Then the sample was stretched, by hand in order to see if the sample gave a response. All samples which gave response were used in further testing.

## 4.2 Replicability test

This replicability test is made to evaluate the differences between produced samples. Additionally, the test was conducted to evaluate the replicability of the produced samples and estimate the reliability of the sensor. The test is conducted in quantitative measures and random sampling. The test was conducted in a reometer "Physica MCR 500" from Paar Physics situated at the Swedish School of Textile in order to achieve the exact strain and frequency to enable the same test conditions.

10 meters of pre-shrunk bicomponent PVDF was taken and cut into pieces of 1 meter. One sample of 20 cm was cut out of every 1 meter piece at random origin. The origin was determined with a random number generator. The cut samples were coated with Elastosil® LR 3162 A/B according to the instructions concerning coating and connecting the inner electrode in section 4.1.2. The coating was placed in the middle of the sample with the length of 15 cm leaving 2.5 cm of uncoated yarn on each side. All samples were coated with masking tape to ensure electrical insulation from the rheometer.

Each sample was tested 5 times. During testing a Picoscope was connected to the piezoelectric yarn and the voltage output was recorded. Pre-programmed settings made for testing fibers was used in the software for the reometer. The settings used were: an increase of momentum of 4 mNm until stretched, the applied momentum of 2.8 mNm with the frequency of 5 Hz. The mean value (MV) from each testing curve was used in further calculations.

### 4.2.1 Testing in low pH

The application area which is the bowel has harsh conditions considering pH. A simple test was conducted to record if a low pH affects the piezoelectric PVDF fiber and the coating. 3 glass beakers were filled with 200 ml of 30% hydrochloric acid in each. The pH was measured with litmus paper to ensure a pH of 1. 3 different samples were made. Sample 1 was the piezoelectric PVDF yarn which was cut into a piece of 10 cm. Sample 2, a coated piezoelectric PVDF fiber of 10 cm. Sample 3, a square of the coating. Each sample was placed in a beaker which was enclosed and left for 24 h. The samples were after 24 h taken from the beakers and dried in room temperature.

Two different tests were conducted when the sample had been in acid for 24 h:

- Rubbing with a paper onto the surface
- Strain until breakage

The evaluation was done ocularly. Each sample was compared with an untreated sample of same sort and evaluated from each other.

### 4.3 Textile structures

The structures used in this study have a resemblance of a grid with the pattern of a loose plain weave. The construction was chosen due to a grid has the same pattern as a coordinate system, giving the warp a y-axis and the weft an x-axis. When there is more than 2 points in a reference system a 3D image is possible to project. The same theory can be applied on a square where the number of points increases from 3 to 4. If the reference point shown in figure 7, while measuring has the value zero and the remaining points have different values from the reference point a “height” difference can be estimated when considering the value of the reference point. Giving a 2D grid, which is bent in the third dimension. The evaluation method is used during measurements of the two different structures described in following sections.

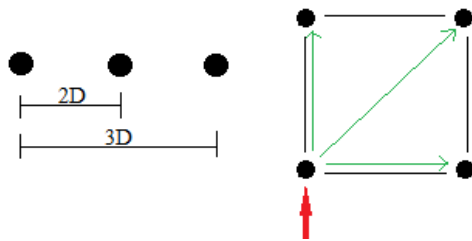


Figure 7 The figure to the left defines how many points needed to illustrate a 3 dimensional structure. The figure to the right shows how the reference point (where the red arrow is pointed) is related to each corner in a square when in a coordinate system. By relating the reference point to the other three points (corners) shown with green arrows in the figure, a 3 dimensional projection of a reference system is possible.

All samples in the following sections which were integrated in a structure had a copper thread connected to the outer electrode. The copper thread is extension of the outer electrode when tested to avoid strain from testing equipment. One copper thread was used for each piezoelectric PVDF yarn.

#### 4.3.1 First sample

In order to test if it is possible to make a useful coordinate system of a piezoelectric PVDF fiber a test sample called sample 0, with 4 piezoelectric PVDF yarns making a square was done. Sample 0 was made with 4 PVDF fibers prepared according to section 4.1 with dimensions of 10 cm yarn and 5 cm of coated area. The 4 yarns were placed on a carrier of a plain weave mosquito net as shown in figure 8. In order to place and keep them in a strained position, all yarns were sewn onto the carrier in the structural pattern of a plain weave and a square.

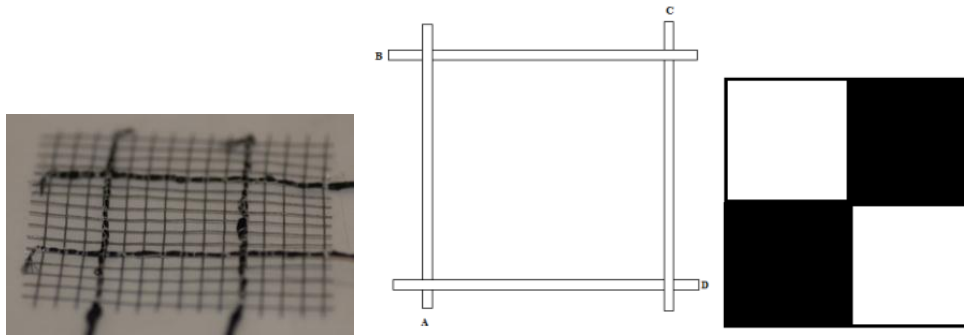


Figure 8 The picture to the left displays the Sample 0. The illustration in the middle the numbering of all yarns which are used in further testing and the figure to the right is the plain weave pattern.

Sample 0 was then tested placed on two different surfaces, one hard and one elastic foam. The hard surface was a plain painted wooden area. The elastic foam surface was a laminated 2 layered structure where the bottom is a carrier and the second layer is foam. The height of the foam was 1 cm and the maximum compressed height of 0.3 cm. Both surfaces were tested with the same method separately. In order to apply pressure a force of 5 N was used to apply a circular weight with a diameter of 1 cm on one corner at a time as shown in the table 1 below. All four yarns were recorder when each corner was tested.

Table 1 Testing matrix of sample 0.

	A	B	C	D
Test 1	X			X
Test 2	X	X		
Test 3		X	X	
Test 4			X	X

#### 4.3.2 Integrated textile structure

Following section 4.1 6 yarns was prepared. The dimensions of the PVDF yarns were 50 cm and the coated are was situated 1 cm from one end. The coated area was 8 cm long for 2 yarns and 3 cm long for 4 yarns. The bicomponent PVDF fiber was integrated by hand using a crochet<sup>9</sup> process in the stent structure with the resemblance of a plain weave. As seen in figure 10 in the box at the upper left corner the fiber was integrated in a manner of one up and one down throughout the stent structure. In larger perspective the fibers were placed to one another as a plain weave. There were 2 horizontally placed yarns and 4 vertically placed yarns. The 2 yarns with longer coating were placed horizontally and the 4 yarns with shorter coating were placed vertically. Each yarn was fastened with Superglue Precision at the ends as shown in figure 10 with green arrows. The yarns were in a strained position, meaning no loose loops, in order to enable measuring compression. The dimensions where 20 x 20 mm  $\pm$  1 mm of each square. The

<sup>9</sup> A crochet process can be defined as using a needle much alike the needles used in the knitting process to create a loop and interloping with another loop, though in this case only making half the process meaning making a loop but then instead of a new loop draw the yarn all the way through the first loop.

longer uncoated ends of each yarn were drawn inwards to the center of the stent and gather in a small tube to prevent entanglement. The copper wires used to extend the outer electrode, were cut 50 cm long.

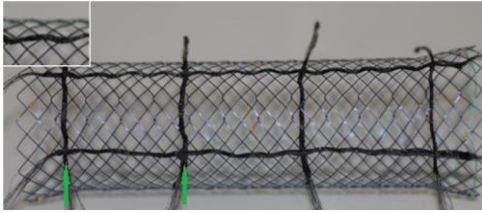


**Figure 9** A display of how the PVDF fiber was integrated in the stent. The PVDF fiber was fastened with glue to where the green arrow is pointing in order to keep them in place during movement and keeping them strained and avoid displacements or unraveling. Small bow to the left shows how the fiber was integrated.

#### 4.3.3 Secondary textile structure

All fibers were prepared as described in section 4.1. There were 6 samples made with the dimensions of PVDF fiber being 50 cm long. The coated area was situated 1 cm from one end. The coating was 8 cm long for 2 yarns and 3 cm long for 4 yarns. The yarns were sewn by hand with a thin overlock thread Synton onto a carrier made of a plain weave mosquito net. There were 2 horizontally placed yarns and 4 vertically placed yarn. The 2 yarns with longer coated area was used for the horizontally placements and the 4 shorter for the vertical placement. The carrier weave is used to make the construction more stable and keep the yarn strained and preventing loose loops. The construction can be seen in figure 10 in the upper corner to the left. The dimensions were  $20 \times 20 \text{ mm} \pm 1 \text{ mm}$  of each square. The whole construction was sewn onto the stent with small stitches with the Synton, in the meeting points of the PVDF yarn as shown in figure 10 with green arrows. All longer ends were drawn through the stent to the center and gathered in a small tube to avoid entanglement. To connect the outer electrode to the Picoscope a copper wire with the length of 50 cm was used.

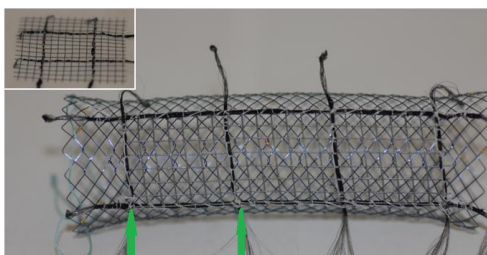


**Figure 10** A plain weave as a carrier for the piezoelectric PVDF fiber sewn onto a stent. The green arrows show the fastening points for the secondary structure. The box in the upper left corner shows the secondary structure before fastening.

#### 4.4 Methods for simulating bowel movements

In order to characterize the response from the piezoelectric PVDF fiber 2 methods for simulating bowel movements were developed. These are presented in detail below. For both test methods a wooden cradle was used. A tube made of an elastic rubber was used as an alternative for a bowel. The cradle's openings for the tube

were slightly smaller than the tube in order for it to stay in place. The tube was cut in a length where approximately 1.5-2 cm on each side of the cradle was sticking out. While testing, the tube was in a stretch condition, meaning the tube was not bending anywhere inside of the cradle. Additionally, clamps were used to fasten the elastic tube to each side of the cradle. The testing method ring compression was fastened with an additional rack for stabilizing the setup. The testing method ring movement was not fastened with any additional clamps. Both of the named methods are described in following sections 4.4.1 and 4.4.2.

#### 4.4.1 Ring compression method

The bowel mainly has muscle contractions to push the content of the bowel forward to simulate the motion a ring compression test was developed. All the engineering drawings can be found in Appendix A with the dimensions of each part. Additionally, some of the dimensions are used in the calculations of the torque<sup>10</sup>, force<sup>11</sup> and pressure<sup>12</sup>.

A compression with the compressed shape of an oval, while in rest, a perfect circle was made with one side movable and the other non-movable. A lever is used to push a metal piece forward which presses the movable piece forward causing compression of the stent. In order to apply force on the lever, a dynamometer was hanged in the outer part of the lever. More details of where and dimensions can be found in the drawings in Appendix A. As seen in figure 11 the dynamometer is placed in a position where it draws the lever upwards, giving strain to the stent.

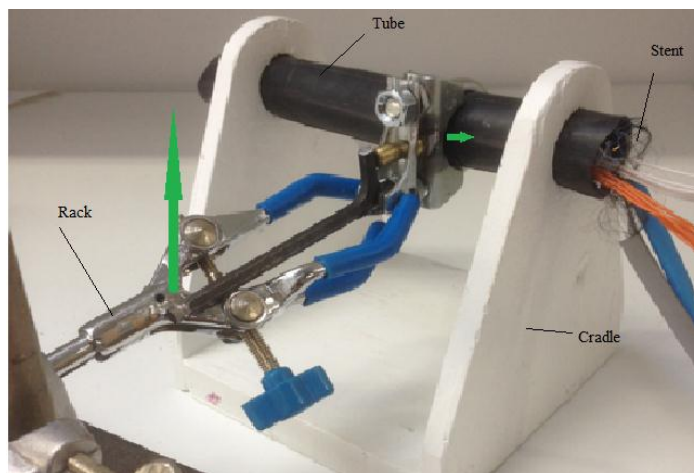


**Figure 11** A display of how the method was set-up. In the actual testing the stent is not as far out to the side as it is in this picture, it shows only to understand the assembly. The large green arrow represent where the force  $F_1$  is applied and is measured with a dynamometer.

<sup>10</sup> Torque is defined as  $\tau = r \times F$  where  $F$  is the force vector,  $r$  is a vector and the distance from where the force is applied and the torque is measured which gives that  $\tau$  is the torque vector. (Serwey & Jewett, 2013)

<sup>11</sup> The force  $F$  is defined as follows:  $F = ma$  where the  $m$  is mass and  $a$  is the acceleration. (Serwey & Jewett, 2013)

<sup>12</sup> The pressure can be defined as follows  $P = \frac{F}{A}$  where  $F$  is the applied force and  $A$  is the area of which the force is distributed over. (Serwey & Jewett, 2013)

In order to understand how much force and pressure was applied on the stent, additionally following calculations, an approximation was done. The measurement of the lever can be found in the sketches for the testing device in Appendix B. The relationship for the force applied  $F_1$  and force transmitted  $F_2$  can be approximated as follows with figure 12, a simplified reference drawing. All friction forces were ignored.

When  $F_1$  is measured with a dynamometer in neutral position:

$$F_1 = 0,08 \text{ N } m_1 = 6,1 \cdot 10^{-4} \text{ kg, and } m_2 = 7,5 \cdot 10^{-3} \text{ kg}$$

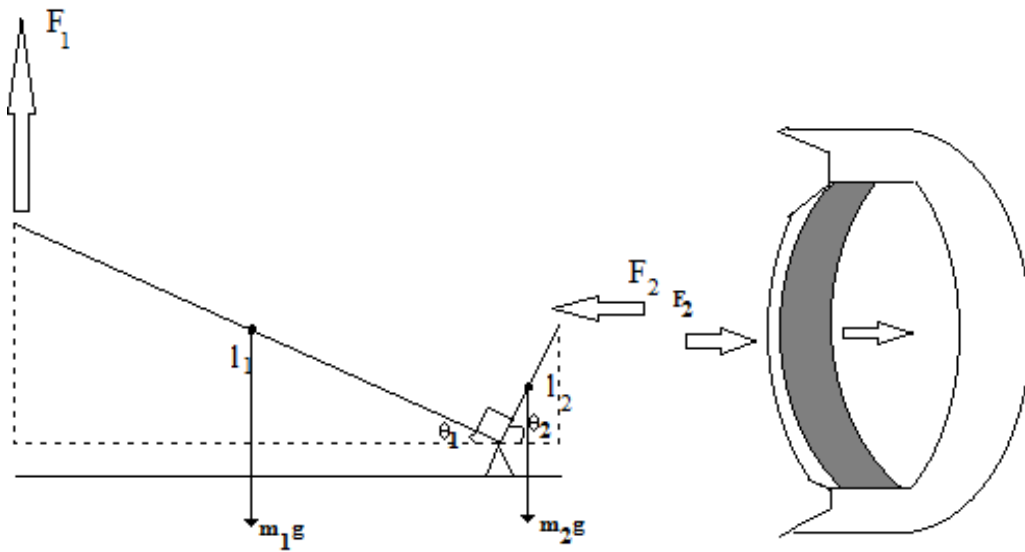


Figure 12 The relation while force is applied to the lever to the left. The force distribution of the force , the pressure when acting on the stent is displayed in the figure to the right colored with grey.

The following equation is retrieved from figure 14

$$\frac{F_1 \cdot l_1 \cos \theta_1 + m_2 g \frac{l_2 \sin \theta_1}{2} - m_1 g \frac{l_1 \cos \theta_2}{2}}{l_2 \cos \theta_2} = F_2 \quad \text{Eq. 1}$$

The applied  $F_1$  when testing were  $10 \text{ N} \pm 0,5 \text{ N}$ ,  $\theta_1 = 20^\circ$  and  $\theta_2 = 60^\circ$

The pressure is approximated by calculating the area from the dimensions in Appendix A and is illustrated in figure 15. Where the area is calculated with the measured diameter of 20 mm during compression when  $F_1 = 10 \text{ N}$  giving  $F_2 = 94,4 \text{ N}$  which gives the pressure affecting the stent:

$$p = 190 \text{ kPa}$$

#### 4.4.2 Ring movement method

In order to resemble muscle contractions a ring movement method was done. All engineering drawings and dimensions of each machine part can be found in Appendix B. Some of the dimensions are used in calculations.

Four plastic wheels were fastened in an octagon shaped frame. The metallic frame has one side with the possibility to open. The opening is fastened with a screw and

a screw-nut. All four wheels are mounted freely on its own axis in order for each wheel to move separately. The montage gives the test area where the tube containing the stent is placed. Due to the properties of the montage the stent is compressed circularly. The assembly is displayed in figure 13.

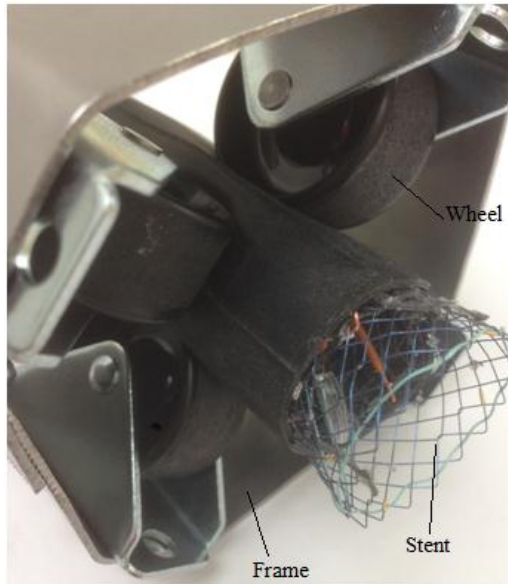


**Figure 13** A display of the ring movement method. The stent is showing only for presentation purposes only. When the method is used in tested the tube is fastened in the cradle and the stent is placed in the middle in length direction of the tube.

The applied force is approximated by taking the force needed in the previous method described in section 4.3.1 to achieve the same diameter which in both cases is 20 mm.

#### **4.5 Testing of the stent**

The yarns were prepared according to sections 4.2.1 and 4.2.2, applied with each structure on each side of the stent. The testing set-up is followed by the scheme shown in figure 14. All tests are described with which yarns are tested and which section the ring compression method device was placed. When both sides are tested the setup for the background is the same but called sample 1 for the integrated structure and sample 2 for the secondary structure. The ring compression method is used in three different sections shown in figure 14 and the ring movement method was rolled horizontal throughout the whole stent. The settings in the software for the PicoScope were; a filtration of 10 Hz and a scale of 1 s/div.

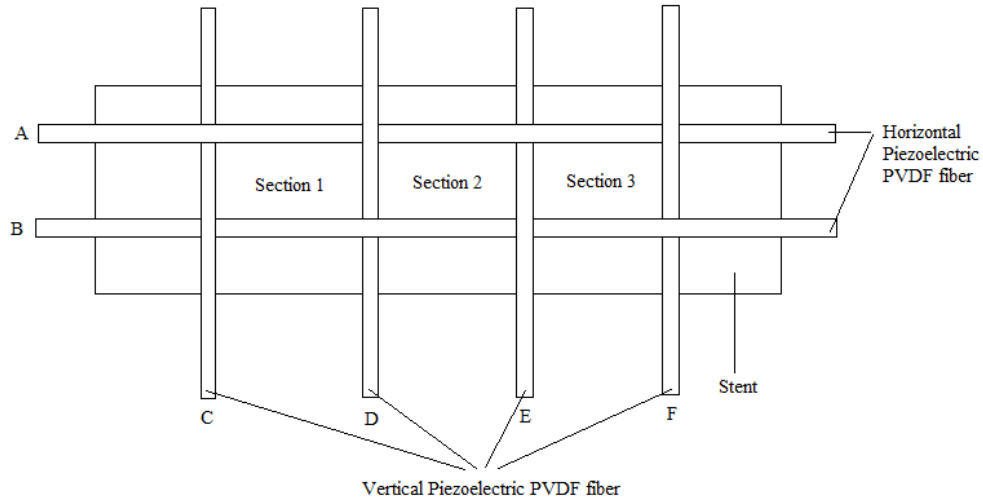


Figure 14 A display of the order of the yarns and placement of the different sections. The setup is used throughout this study.

#### 4.5.1 Test with ring compression method

The test matrix which gives the different testing configurations on sample 1 and 2 with the ring compression method can be seen in table 2 below. Each side is tested according to the matrix and is a one sided test. The number of tests is simplified.

Table 2. Testing matrix for ring compression method

	A	B	C	D	E	F	Section 1	Section 2	Section 3
<b>Test 1</b>	X	X			X	X	X		
<b>Test 2</b>	X	X			X	X		X	
<b>Test 3</b>	X	X			X	X			X
<b>Test 4</b>	X			X	X	X	X		
<b>Test 5</b>	X			X	X	X		X	
<b>Test 6</b>	X			X	X	X			X
<b>Test 7</b>			X	X	X	X	X		
<b>Test 8</b>			X	X	X	X		X	
<b>Test 9</b>			X	X	X	X			X

When both structures are tested, a double sided test, sample 1 has the symbol  $X_1$  and sample 2 has the symbol  $X_2$ . The test matrix with the different test configurations are shown below in table 3. The number of test is simplified from the previous one sided test.

Table 3 Testing matrix for ring compression method when both structures are tested.

	A	B	C	D	E	F	Section 1	Section 2	Section 3
<b>Test 1</b>	$X_1$ $X_2$	$X_1$ $X_2$					X		
<b>Test 2</b>			$X_1$ $X_2$	$X_1$ $X_2$			X		

<b>Test 3</b>			X <sub>1</sub> X <sub>2</sub>	X <sub>1</sub> X <sub>2</sub>				X	
<b>Test 4</b>			X <sub>1</sub> X <sub>2</sub>	X <sub>1</sub> X <sub>2</sub>					X

#### 4.5.2 Test with ring movement method

The one sided test matrix for the yarn configurations on sample 1 and 2 with the ring movement method can be seen in table 4 below. The number of tests has been decreased from the ring compression method due to the rolling motion throughout the horizontal line of the stent which excludes the three regions.

Table 4 Testing matrix with ring movement method

	<b>A</b>	<b>B</b>	<b>C</b>	<b>D</b>	<b>E</b>	<b>F</b>
<b>Test 1</b>	X	X			X	X
<b>Test 2</b>	X			X	X	X
<b>Test 3</b>			X	X	X	X

The test matrix for the double sided test can be seen in table 5. As in section 4.5.1 when conducting a double sided test the different X:s has the same meaning in this section.

Table 5 Testing matrix with ring movement method when both structures are tested.

	<b>A</b>	<b>B</b>	<b>C</b>	<b>D</b>	<b>E</b>	<b>F</b>
<b>Test 1</b>	X <sub>1</sub> X <sub>2</sub>	X <sub>1</sub> X <sub>2</sub>				
<b>Test 2</b>			X <sub>1</sub> X <sub>2</sub>	X <sub>1</sub> X <sub>2</sub>		
<b>Test 3</b>			X <sub>1</sub> X <sub>2</sub>			X <sub>1</sub> X <sub>2</sub>

#### 4.6 Testing after poled in direct contact

The samples from section 4.5 when situated in the stent were poled with direct contact in order to make sure the differences between the points are not irregularities from the in-line poling. The sample was heated to a temperature of 60° C. The outer and inner electrode was connected to HV-Power Supply 0-10 kV from PHYWE. A voltage of 1.5 kV was applied to the circuit during 10 seconds. The ring compression method and the test matrix described in section 4.5.2 were used.

#### 4.7 In vivo

The in vivo test was a part of a larger framework in research of stents at Södra Älvsborgs Sjukhus where there was a possibility to perform an in vivo test. One

pig was used in the in vivo test. The pig was anesthetized during testing. The stent was inserted and placed where the orifice of the stomach was placed in the middle of the stent. In order to increase bowel movements Neostigmin a medicinal preparations was used. The Neostigmin<sup>13</sup> injected intravenously in different concentrations into the pig. Sample 1 was tested during the first injection<sup>14</sup> of Neostigmin. The test configuration of the yarns was A,B, D and E.

---

<sup>13</sup> It is used to reverse neuromuscular blockade induced when anesthetic is used, since anesthetic is often a muscle relaxant. (PharmaCoDane, 2014)

<sup>14</sup> Further information is given after request to the author and/or supervisor

## 5. Result

The results are divided and followed by the order they were described in section 4. Concerning the ring compression method, the ring movement method and the direct poling the main findings are presented. The results which are not displayed in section 5 can be found in Appendix C-E to completion. The curves are decreased to manageable size, where the output is visually comprehensible. All yarns were connected numbered from the bottom and up after the numerical order of the letters.

### 5.1 Pre-shrinking

The yarn was measured pre-heating and post-heating in 120° C. The total mean value (MV) for the 10 yarns were 85.25 cm giving a shrinkage of 14.75%.

### 5.2 Replicability test

Each yarn was tested 5 times and the mean value from each curve was taken. A MV from the 5 test was then calculated for each yarn and is displayed figure 15.

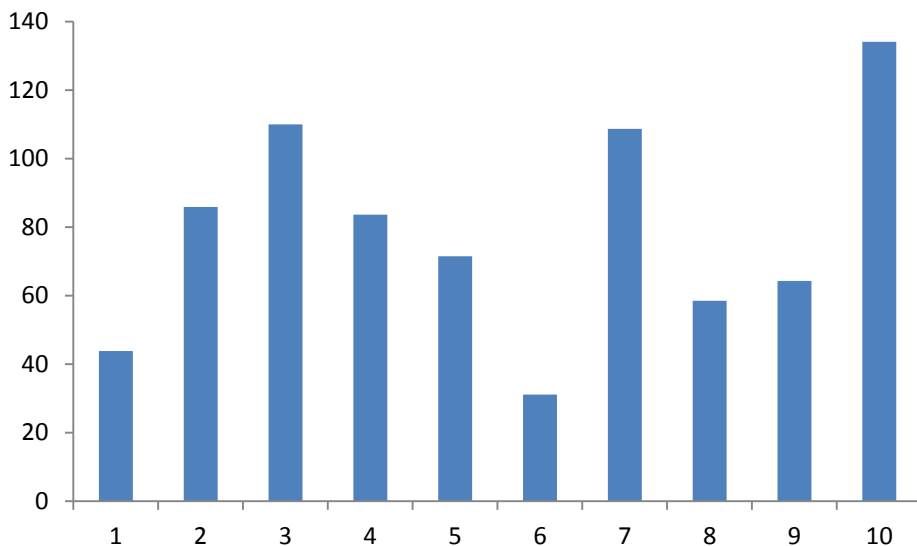


Figure 15 The individual MV of each tested yarn. Where the yarns are represented in the x-axis and the total MV of each yarn are represented in the y-axis.

#### 5.1.2 Testing in low pH

The samples were exposed to hydrochloric acid with pH 1 during 24 h. In table 6 the test result from the two testing methods are displayed. The evaluation was conducted ocularly.

Table 6

Sample	1	2	3
Rubbing	Clean paper	Some CB stained the paper	Some CB stained the paper
Strain until breakage	More brittle	Slightly more brittle	Slightly more brittle

### 5.3 Sample 0

One test result is shown here and the remaining test results can be found in Appendix C. Settings for the PicoScope: a filtration of 10 Hz and a scale of 1 s/div. The x-axis is divided into seconds, where one square is one second. The y-axis is divided in mV where one square is 20 mV. Where all yarns had the same connections through the test and where numbered starting with A from the bottom blue curve.

Test 1 on a hard surface where corner made of yarn A and D was tested. Where yarn A and D gives a voltage output and place the origin of the signal in the corner where yarn A and D meet.

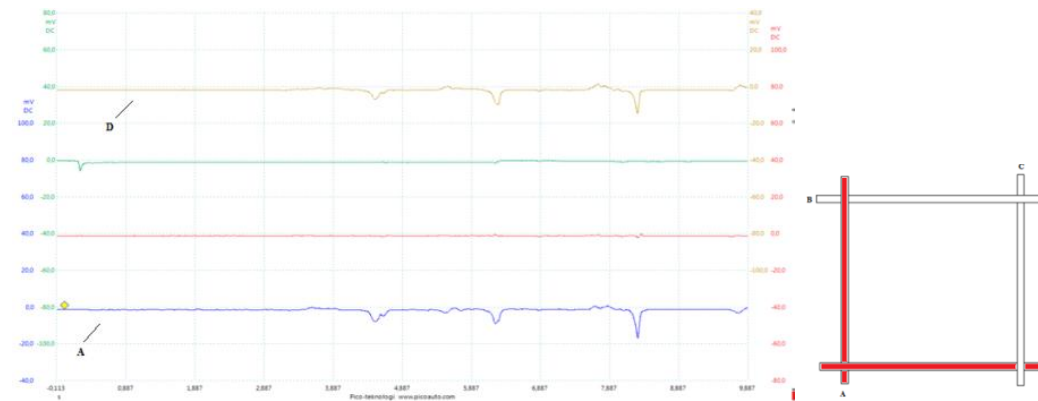


Figure 16 Test 1 hard surface, where the test was in the corner of yarn A and D

Test 1 on an elastic foam surface, where the test conditions is same as above, giving the origin of the signal where yarn A and D meet.

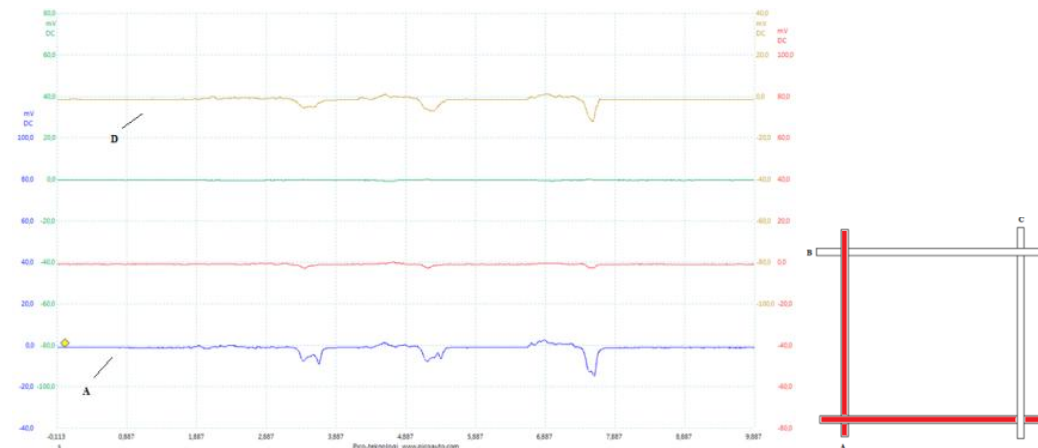


Figure 17 Test 1 squasy surface, where the test was in the corner of yarn A and D

### 5.4 Ring compression testing

The samples were tested according to the ring compression method with an applied force of  $10 \text{ N} \pm 0,5 \text{ N}$ .

### 5.4.1 Sample 1

Some of the resulting curves are displayed below. The result which is not displayed here can be found in Appendix D. Settings for the PicoScope: a filtration of 10 Hz and a scale of 1 s/div. The x-axis is divided into seconds, where one square is one second. The y-axis is divided in mV where one square is 20 mV.

In figure 18 below test 1 is displayed. Where the two bottom curves give a clear signal on the horizontal yarns where the actual pressure is and the two upper curves, the vertical yarns gives a slight signal.

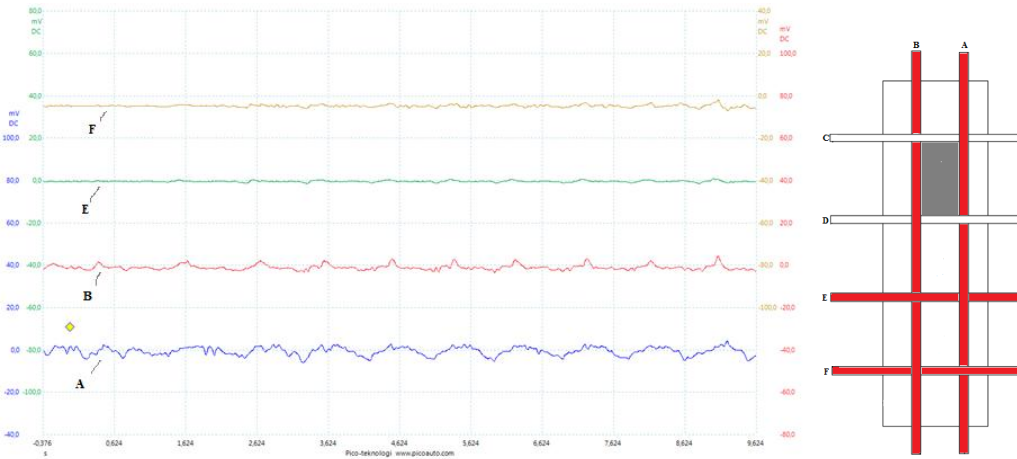


Figure 18 Test 1 Where the yarns A, B, E, and F are tested in section 1.

In figure 19 below test 4 is shown. Where the bottom curve the yarn A gives a clear signal where the pressure is in the horizontal yarn and the vertical yarns has a small signal.

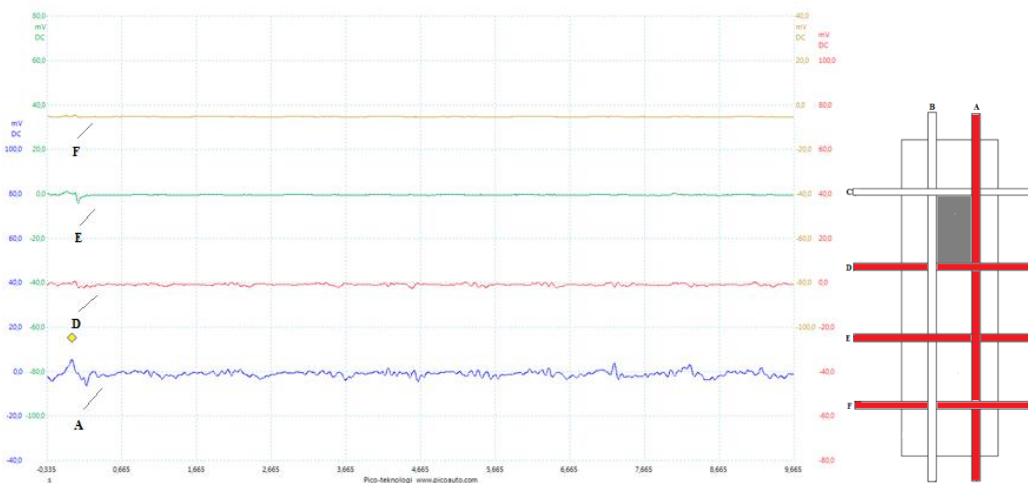


Figure 19 Where the yarns A, D, E, and F are tested in section 1.

In figure 20 below test 7 is displayed. Where all curves show small output signal. None of the yarns has a direct pressure.

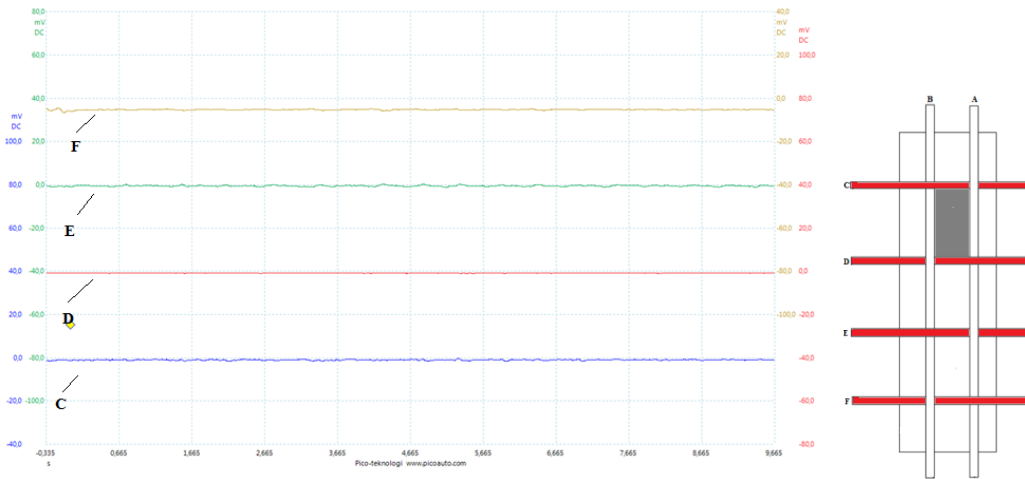


Figure 20 Where the yarns C, D, E, and F, is tested in section 1.

### 5.4.2 Sample 2

A few result are presented in this section, the remaining can be found in Appendix D. Settings for the PicoScope: a filtration of 10 Hz and a scale of 1 s/div. The x-axis is divided into seconds, where one square is one second. The y-axis is divided in mV where one square is 20 mV.

Test 1 is shown below in figure 21. The horizontal yarns A and B which are the two bottom curves gives a higher output signal where the pressure is than the vertical yarns which are not affected directly by the pressure.

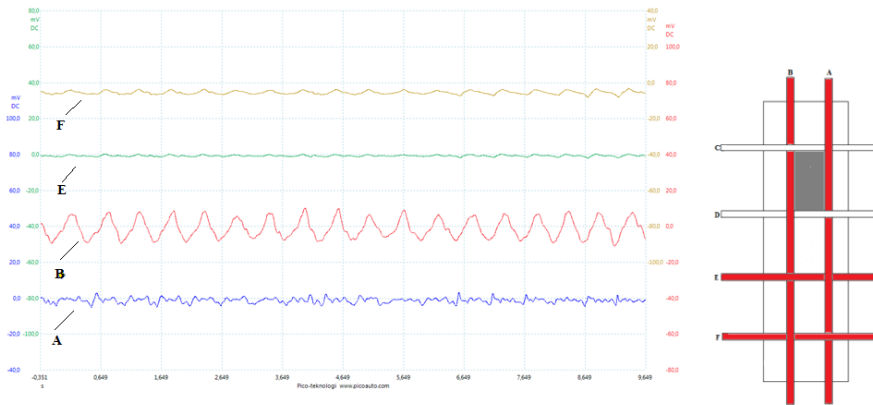


Figure 21 Where yarns A, B, E, and F which are tested in section 1

Test 4 is shown below in figure 22. Where the bottom curve is the horizontal yarn A giving a higher output signal due to the direct pressure compared to the vertical yarns D, E and F which is not affected to direct pressure.

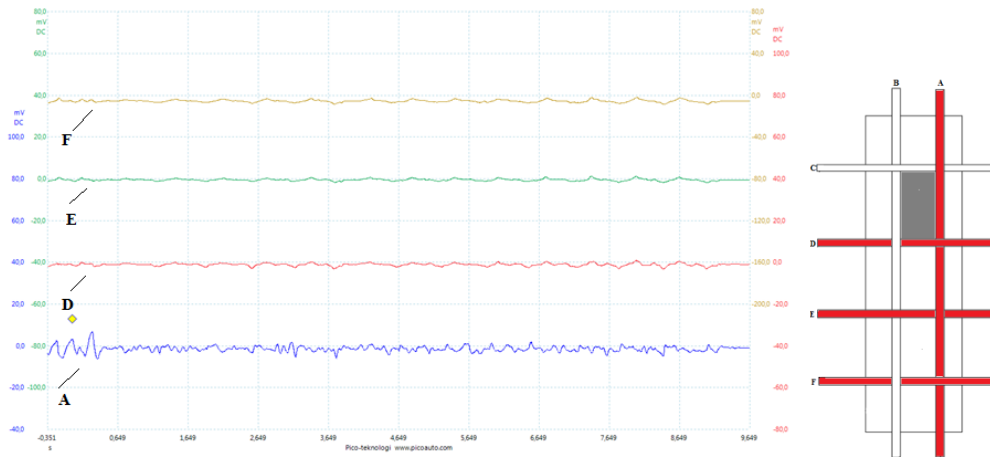


Figure 22 Where yarns A, D, E, and F which are tested in section 1

Test 7 is displayed in figure 27 below, where all vertical yarns have an output signal. None of the yarns is affected by a direct pressure.

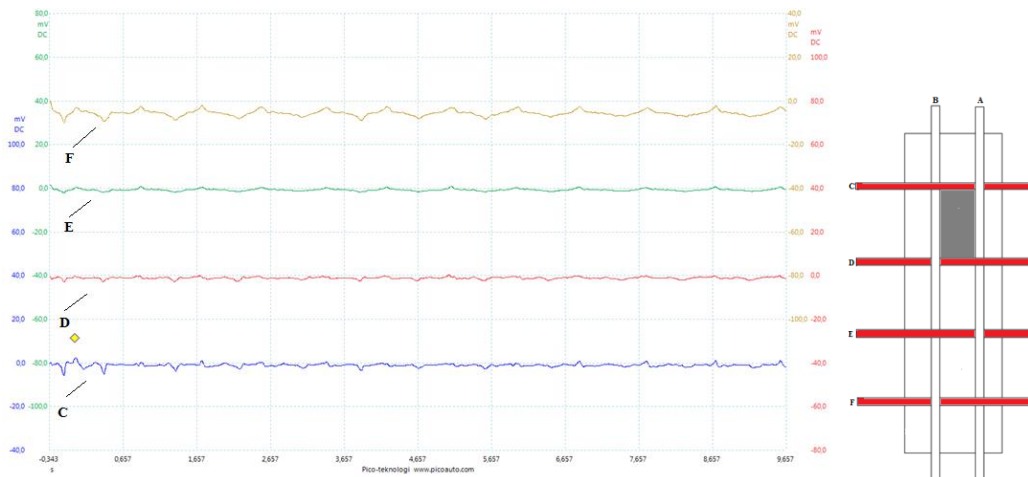


Figure 23 Where yarns C, D, E, and F which are tested in section 1

### 5.4.3 Double sided test

Two of the tests are displayed in this section and the two remaining can be seen in Appendix D. The numbering of the test are the same as in the initial testing matrix described in section 4.5.1. Settings for the PicoScope: a filtration of 10 Hz and a scale of 1 s/div. The x-axis is divided into seconds, where one square is one second. The y-axis is divided in mV where one square is 20 mV.

Test 1 is displayed below, where both of the horizontal yarns in sample 1 and 2 are tested. Where the first A and B from the bottom are sample 1 and the second A and B is sample 2.

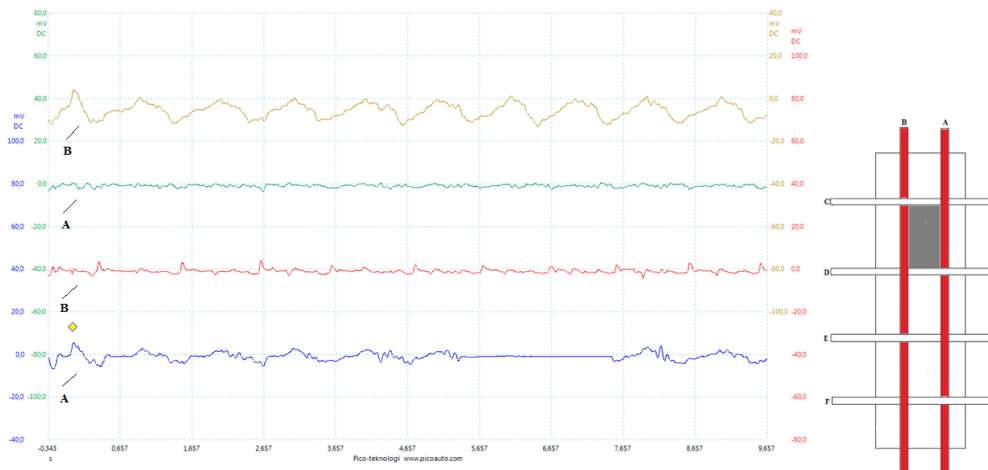


Figure 24 Where yarns A and B in both structures are tested in section 1.

Test 2 is displayed in figure 25 below where yarns C and D are tested simultaneously in both sample 1 and 2. Where the first C and D from the bottom is sample 1 and the second C and D is sample 2.

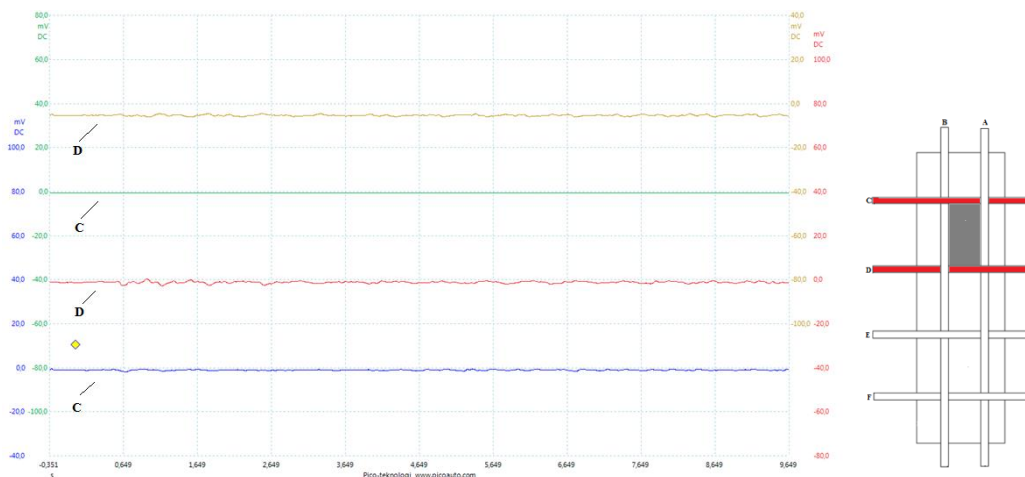


Figure 25 Where yarn C and D is tested in sample 1 and 2.

## 5.5 Ring movement testing

The samples were tested according to the ring movement method. The placement of the yarns is described in section 4.5.

### 5.4.1 Sample 1

One test of three tests is displayed here and the two remaining can be found in Appendix E. Settings for the PicoScope: a filtration of 10 Hz and a scale of 1 s/div. The x-axis is divided into seconds, where one square is one second. The y-axis is divided in mV where one square is 20 mV.

Test 1 is shown in the figure 26 below where the 2 lower curves are the horizontally placed A and B yarns which has constant pressure from the ring method and the two upper curves represent the vertically placed yarns E and F. The green curve yarn E has an output voltage before the brown curve yarn F. The displacement of yarn F gives a origin of the signal in the structure.

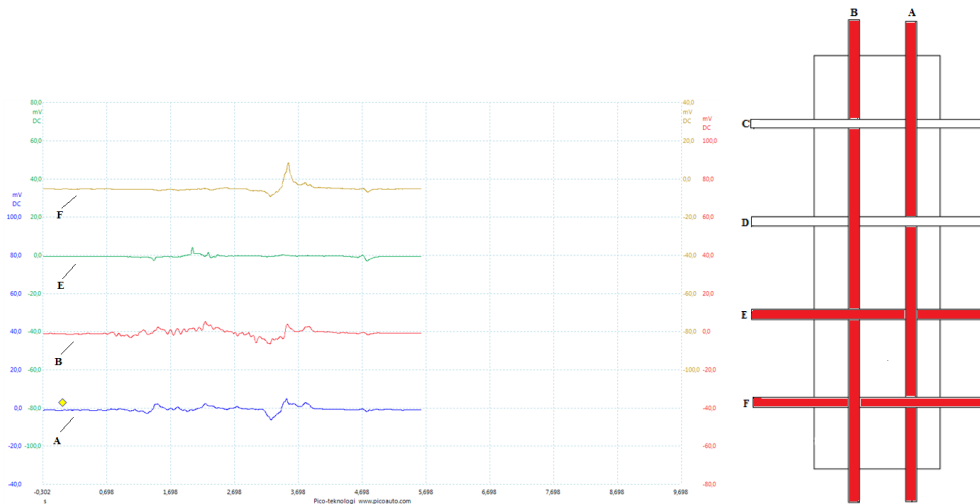


Figure 26 Where the yarns A, B, E and F are tested from the left side.

### 5.4.2 Sample 2

It is only one test which is displayed here and the two others can be found in Appendix E. Settings for the PicoScope: a filtration of 10 Hz and a scale of 1 s/div. The x-axis is divided into seconds, where one square is one second. The y-axis is divided in mV where one square is 20 mV.

Test 1 is shown in figure 27 below, the 2 curves in the bottom represent the horizontally placed yarns and the 2 curves in the upper part represent vertically placed yarns. The displacement of the brown curve yarn F compared to the green curve yarn E gives the origin of the signal in the structure.

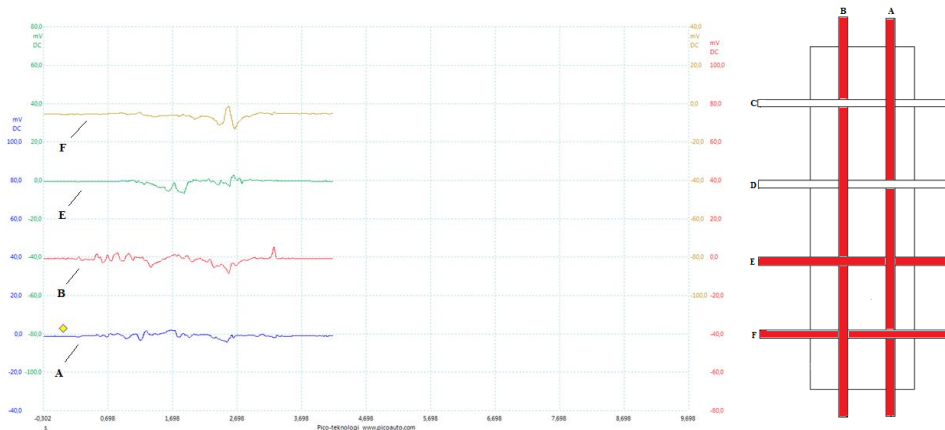


Figure 27 Where the yarns A, B, E and F are tested from the left side.

### 5.4.3 Double sided test

One test was chosen to be displayed here and the remaining can be found in Appendix E. The x-axis is divided into seconds, where one square is one second. The y-axis is divided in mV where one square is 20 mV.

Test 1 where yarn A and B in both structures are tested. Where the first A and B from the bottom are sample 1 and the second A and B is sample 2.

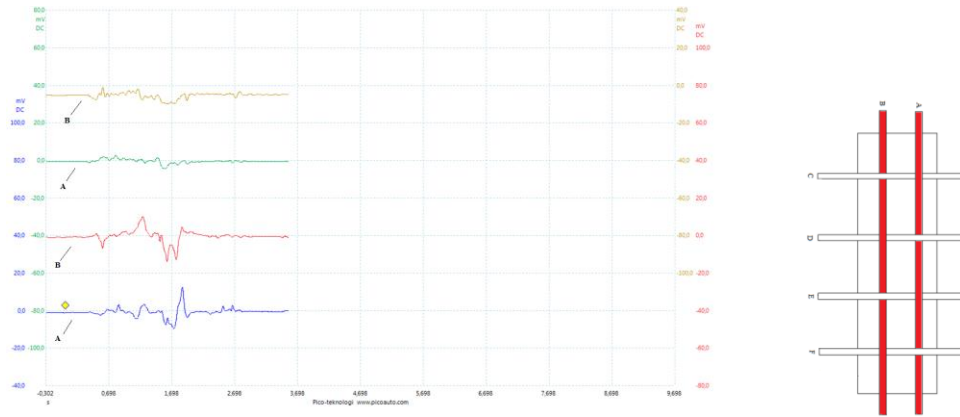


Figure 28 Yarn A and B are tested

### 5.6 Testing after poled in direct contact

The two first test, test 1 and 2 from the ring compression method tests are displayed, due to they are same as for the in-line poled sample, but higher response a smaller amount is shown. Settings for the PicoScope: a filtration of 10 Hz and a scale of 1 s/div. The x-axis is divided into seconds, where one square is one second. The y-axis is divided in mV where one square is 20 mV.

Test 1 where yarns A,B, E and F is tested. Where the displacement of the brown curve (yarn F) compared to the green curve (yarn E) gives the origin of the signal in the structure.

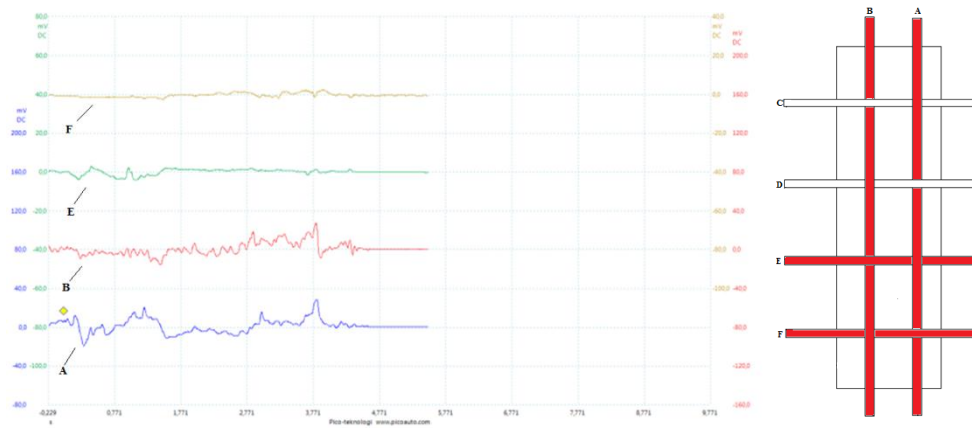


Figure 29 Yarn A, B, E and F is tested

Test 2 where yarns A, D, E and F are tested. Where the displacement of the green curve (yarn E) and brown curve (yarn F) compared to the red curve (yarn D) gives the origin of the signal.

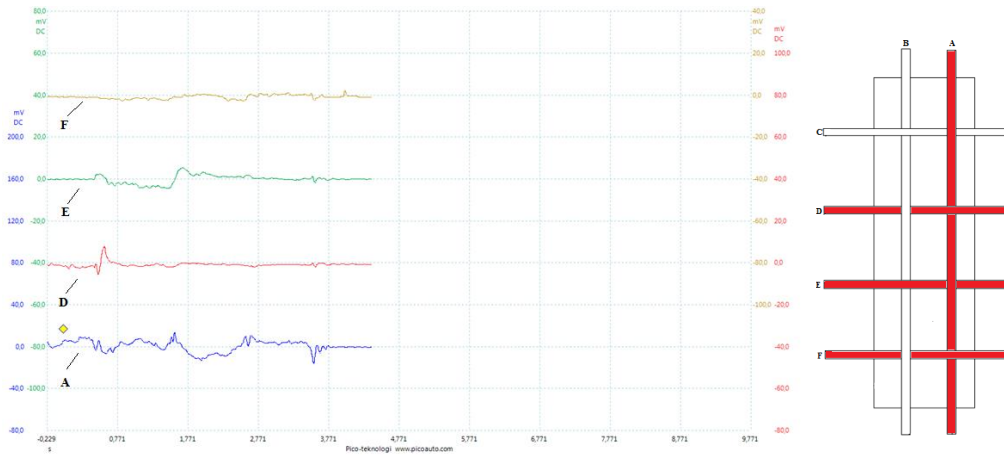


Figure 30 Yarn A, D, E and F is tested

### 5.7 In vivo testing

The stent was placed in the orifice of the stomach, where yarns A, B, D and E were tested after injection of Neostigmin. It was also observed that the breathing did not disturb the recorded data. The x-axis is divided into seconds, where one square is 10 seconds. The y-axis is divided in mV where one square is 20 mV. Where a larger voltage output can be seen on the horizontal yarns A and B compared to the vertical placed yarns D and E.

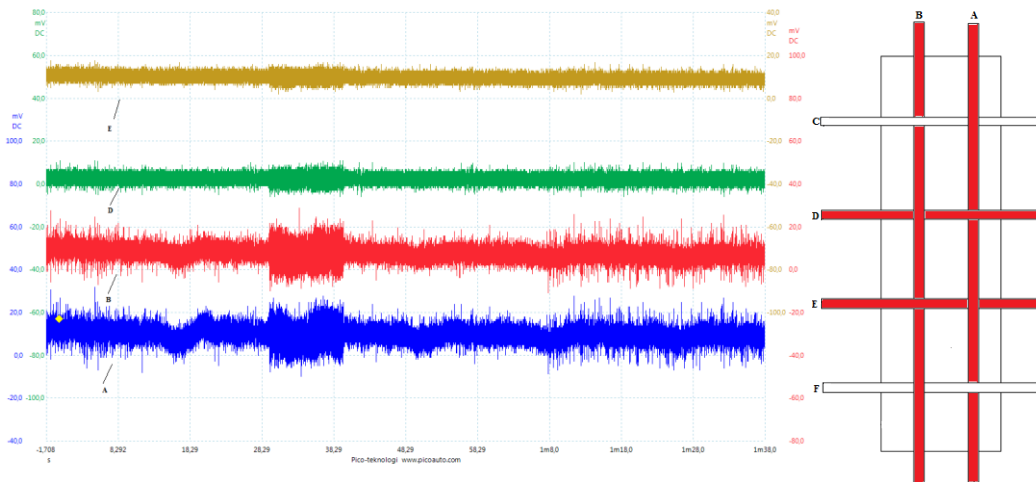


Figure 31 Test 1 where yarns A, B, D and E was tested. Where the numbering of the yarns started from the bottom blue curve with yarn A.

## 6. Discussion

In the following sections within this chapter, relevant aspect of this study is discussed and analyzed further.

### 6.1 Shrinkage test

During preparation for the replicability test the fibers during heating started shrinking. When discussed with Anja Lund and looking through literature the phenomena had not been observed before. A test was conducted in order to see how much the fiber actually did shrink. The result was unexpectedly high causing the decision of preheat all further samples. It was observed that if the shrinkage and fixing of the coating was done at the same time, the sample would not be even, due to the uneven shrinkage of each filament. The uneven shrinkage gave loops and a very uneven coated sample. The uneven sample gave a decreasing curve while in the reometer. The shrinkage might have been due to the exclusion of the last wheel in the solid state drawing to enable a continuous in-line poling. Also the settings during production the used samples were different since the SSDR was almost half compared to other studies.

### 6.2 Textile structures and sample selection

The largest problem with applying a piezoelectric fiber in a textile structure is the flexibility of the textile structure used. The simple definition of a piezoelectric fiber gives some answers; in polarization proportional to the applied strain (Tichý J. et al., 2010). But it is only the strain when the fiber is stretched which gives the output. Straightening of crimp caused by the textile structure used which is shown in figure 32 does not give any output. This gives a complexity of applying a piezoelectric fiber in a textile structure. A possibility could be embroidery, but then the sewing area might be too small, due to a majority of all embroidery machines cut of the thread between motifs enabling small sewing areas. It is not an ideal application method for a piezoelectric fiber. Due to problematic of the formation of crimp the piezoelectric fiber might not be suitable to be integrated in a larger elastic structure.

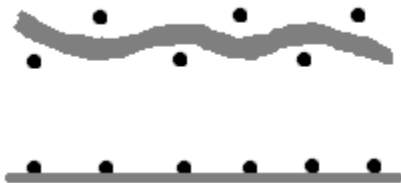


Figure 32 Upper figure displays a plain weave where the structure enable crimp and the bottom figure display the more efficient way of inserting the fiber. Though, the structure below is not a weave since the warp and weft does not *interlace*.

The structures was based and inspired by a conventional simple plain weave mosquito net. The initial idea was to make a loose plain weave of the piezoelectric PVDF fiber in both the weft and warp creating a structure resembling a coordinate system which could be used as a sensor system in any application. The grid

structure was also chosen due to the property of being less elastic than a knitted structure. The first construction is unfortunately, since it is integrated in the structure and individually designed depending on type of the stent a very manually processed structure. The second structure's purpose was to make a structure which could work in symbiosis with the stent and measuring the bowel movement. But the second structure could also be used as a generic structure on the covered stents and in any application where compression needs to be measured.

The evaluation between the 2 structures was done ocularly in the given curves. The mean value is not an optimal evaluation since in the ring movement method the displacement of e.g. the forth curve compared to the first is the actual result.

### **6.2.1 Sample 0**

Sample 0 was chosen in order to see if the theoretical reasoning of creating a coordinate system to place the origin of the signal was possible when used on a hard and squashy surface. At first, the sample was actually done as a plain weave structure by hand. But the coating process made the system unstable, the coating was intended to keep the yarns in place which when applied by hand was not the case, due to the process ability of the coating. It is difficult to apply the coating due to the viscosity. Also the strain of the fiber was not satisfying and reducing the size was not an option. Instead a carrier, in the form of plain weave mosquito net was chosen and the piezoelectric PVDF yarn was sewn on by hand. The testing showed that it worked due to the low voltage output from the yarns forming the corners which was not tested.

### **6.2.2 Sample 1**

The structure of sample 1 was chosen due to the theory that the piezoelectric yarn would follow the stents movement during compression in a higher degree than when applied as a secondary structure on top of the stent. The yarns was still in a plain weave construction but had to be glued in the meeting points in order to keep the strain. Making a knot in each did not work in order to keep the fiber in place. Though, the fibers when in placed had some crimp when the stent was in neutral position. By gluing the meeting points the thought was to keep a strain while the stent was subjected to compression.

### **6.2.3 Sample 2**

The structure of sample 2 was chosen due to the already discussed theory of making a plain weave. From the beginning the yarn was loosely sewn onto the carrier, though when testing few or none signals were recorded. Due to the low output more stitches were used which also gave a higher output when using the developed test methods.

## **6.3 Material selection**

In this study PVDF was used due to its possibility, compared to PLA, a more environmentally friendly fiber, can withstand harsh conditions in the bowel e.g.

pH 1. PVDF is also the polymer known to have the highest piezoelectric effect. (Hottle, Bilec, & Landis, 2013) Early in the study the choice was to use a continuously made, meaning an in-line poled piezoelectric fiber, merely due to the fact that the only available at that time was an in-lined poled fiber. But the major reason was to investigate whether or not a continuous textile processed piezoelectric PVDF fiber was ready for applications.

The reason a carrier was used in this study was merely due to the aim of the study: measure dynamic compression. Not to develop a perfect coated plain weave by hand. The chosen mosquito net was used due to its structure, the even weave which was coated giving few or none displacements of yarns during shearing forces. This meant a very stable and form stable structure to work with during this study.

Only one sort of stent was used in this study, an open, since it is easier to integrate fibers in an open structure. But also due to the fact that there are several different stent with different properties making the actual characterization of the piezoelectric PVDF fiber more complex than it had to be.

The choice of using a silicone coating as an outer electrode was merely due to remove the obstacle of having a liquid resembling gastric juice with a pH 1 inserted in the testing tube while using the test methods. The difficulty while testing would increase and the safety decrease. The choice went to the conductive silicone rubber Elastosil® LR 3162 due to its high conductivity and has been used successfully in previous research on Swerea IVF and the Swedish School of Textile.

#### **6.4 Construction of testing methods**

The possibilities of actually testing a piezoelectric fiber itself and when it is integrated are fairly limited at the Swedish School of Textiles, especially for an application such as a stent. Sure a tensile tester could be used, which is available at the school. But the tensile tester applies the force evenly across the stent and during a long time interval. Also the reometer could be used, which it was for the replicability test, due to it was possible to set a fixed torque and the frequency. Though, the problem with the reometer was the inability of testing the fibers when integrated in a stent. The conditions in the bowel does not resemble the movements these machine offers.

In order to have test conditions similar to the bowel two methods were developed to achieve a testing and evaluation serving the purpose of measuring bowel movement. The test methods were inspired by the movement of the bowel, both by theoretical reading and discussing with the consulting surgeons since they have seen actual bowel movements. But there is no certain way of knowing if it actually is a good testing method for the specific application as in the bowel since the area is much unexplored.

A further development of both test methods would be to combine them. The new design would be by using the ring compression method and add a hydraulically pressure to each wheel separately. The new design enables separate control and pressure from each of the wheel giving a more dynamic pressure control but also more ways of testing the piezoelectric PVDF fiber and different stent designs. The more dynamic and the resemblance a test method has to the actual environment it's trying to resemble the better the result is in order to understand the complexity. The method would also be easier to apply to different stent sizes since it is easier to change the testing diameter.

### **6.5 Applicability of testing methods to different stents**

The test methods were developed in a manor where the differences in mechanical properties between different stent for usage in a bowel where overseen, giving the test methods a very versatile use. They were developed for the specific stents used in the bowel and is not suitable for testing stents e.g. the application area the heart.

There could be a potential problem while testing with the two developed method, since the structure of the stent does not always behave the same way depending on where the pressure is applied. Depending on the reaction of the stent the test results could be different even though one thought it was the same measurement. This can also be seen in the result where the curves for the horizontal placed yarns tend to have higher output signal when testing with the ring compression method. This property is very apparent when comparing test 2 and 3 in the double sided test when using the ring compression method where they should in theory have the same result, due to the symmetry of the stent but they do not. Test 3 gives clearly a higher response compared to test 1. It is also evident when looking at the curve from test 1, sample 1 in the ring compression method that the 2 bottom curves should not in theory vary at all, but due to the structural behavior of the stent they do while testing.

### **6.6 Replicability test**

The measured differences can be due to a number of things. Since the fiber is spun according to a conventional textile process the errors compared to laboratory made fibers could be huge e.g. the fiber which was used in this study had a significant smaller SDR of 2.3 to the comparable laboratory made with a SDR of 4. Due to this the fiber might not have the same ratio between core and sheat, giving different properties. It is also possible that the core, which was observed while handling the fiber is not connected everywhere in e.g. a meter of filament, causing a shortcut giving the whole yarn of 24 filaments different outputs depending on where the breakage of the core occurred.

Making a sensor today of a piezoelectric PVDF fiber is possible but not reliable. There could still be a use even though the fiber is not reliable e.g. before all use each fiber could be characterize of its own interval and then the irregularities in

the intervals could be corrected by a software. Though, this is not economically defensible today since the advantages are less than the costs. The best way for the future of this fiber is to optimize the continuous textile process in order to reduce the irregularities.

### **6.7 Poling in direct contact**

Since the replicability test showed that the irregularities were large of the required batch an direct poling was done in order to reduce one of the errors, the in-line poling. It is possible that the in-line poling gives uneven poling during a continuous textile process. All the yarns where poled in direct contact and then all test in the ring compression and movement test were done again to compare to the previous ones. Due to this the comparison between the two structures is difficult to do because of the structural problematic of the stent as well as the irregularities in the piezoelectric PVDF fiber. The initial thought was that the 2 structures would have more significant differences while measuring than the actual measured response was.

The choice of poling in direct contact was also due to during the initial test it was seen that small forces was not recorder by the fiber. In order to receive any results from the in vivo testing the direct poling was done.

### **6.8 In vivo testing**

During the testing only one structure was chosen to be tested, mainly due to time limitations. The test configurations were reduced after careful contemplation with the surgeons. Additionally due to the placement, in pularus, the orifice of the stomach reduced the test configurations more. The theory during the testing was that the stent used was too strong radially giving difficulties for the pularus to contract properly. Due to smaller compression forces the responses were lower than of the developed test methods. It could also be due to the pig stomach empties in a different interval when considering time and frequency comparing to the human stomach.

The choice of giving Neostigmin was due to when an animal is anesthetized, all bodily functions comes to a rest or goes down in activity, even the bowel movements. By giving the medicine the bowel movement increased enabling measurement of the bowel movement. Unfortunately during the test, the medicine decreased in enabling higher response after each injection. The theory was that the medicine was tiring the bowel.

### **6.9 Evaluation of the developed test methods after the in vivo testing**

It is clear after the in vivo testing that the ring compression method resembles in response to a sphincteric muscle such as the orifice of the stomach. The developed test method is suitable to test sphincteric muscle movements. The other test however cannot be evaluated since downwards contractions caused by the bowel

were never measured while in vivo testing. It is possible that the bowel does actually compress more distributed on the stent while in the bowel than of the ring compression method giving not as clear distinctions between the active sites.

### 6.10 Application in the bowel

The PVDF fiber is from the beginning a hydrophobic polymer and a high chemical resistance. With those properties in mind, the fiber when exposed to a pH 1 during 24 hours would not be affected by the low pH. In this study it clearly shown that PVDF when in fiber form, a low pH gives a more brittle fiber. This phenomena could be due to when the fiber is melt-spun and then drawn in solid state, small cracks in micro scale may have developed. These cracks could then enable the acid to migrate from the surface further into the fiber causing degradation of the fiber. If the degradation has gone too far, eventually the acid would reach the core, the inner electrode. Since the acid is conductive the core would then be in contact via the acid, with the outer electrode causing a shortcut in the circuit. The sensor would then be destroyed and not usable. Additionally the extent of the poling, due to the degradation of the fiber would possibly decrease as well. This was not tested in the low pH since the material is very irregular produced.

On the other hand this unfortunate problem with a shortcut might not be an issue since the main reason for wanting to measure bowel movements is to design the perfect stent. The sensor might only be needed for one week, since it has been shown that the movement of the stent starts already after one week. It is possible that the actual measuring is needed only for a day or two. The measuring data from the short period of time could then be used in a modeling program together with a model of a stent and then simulate what different designs could cause different muscle contractions.

When the piezoelectric PVDF fiber is integrated or used as a secondary structure and with no shielding coating the possibility of mechanical abrasion between the fiber and the metal threads in the stent is increased. Though, this might not be a problem if the actual measuring is a couple of days but if it is longer than it could be another aspect to consider.

It is not intended for the coating to be a part of the actual product since the silicone contains CB. The affects of CB in a living organism is not fully understood and investigated. The CB used in the silicone is supposed to aggregate in order to increase the conductivity of the silicone. Though, the particles in that case would be slightly larger, the problem of having the bowel absorb them and transport them elsewhere inside the body could still exist, since the major function of the bowel is to absorb nutrients in particle size of CB. But the problem would on the other hand not be as large as it would be for e.g. nano tubes of carbon. These have the ability of poking holes in surrounding tissue including the brainstem. This problem of migrating CB could also be a possibility if the PVDF

is allowed to be degraded within the human body since the core contains CB, but not in as high concentrations as of the coating.

Though, when integrated in a stent the fibers are measuring two different things: the normal muscle contractions and the muscle contractions induced by the stent itself. But the stent cannot sense the difference between a “normal” muscle contraction or an induced one. But this is the drawback of any measuring system placed inside or integrated in a stent. On the other hand, the test result may be compared to other measurement done in the bowel which excludes the stent, giving a more nuanced picture of the result.

## 7. Conclusion

In this report it has been shown that it is possible to use a piezoelectric PVDF fiber in order to measure compression when used in a stent for a bowel. The PVDF can be used to place the origin of a signal within a textile structured system.

Due to irregularities in the material the structures cannot be compared to each other. Both structures can be used in order to measure bowel movements. The favorable structure when considering a covered stent, an uncovered stent and a continuous textile process is the secondary structure.

The continuous textile processed in-lined poled piezoelectric PVDF fiber is not yet suitable for making a reliable textile sensor measuring dynamic compression.

## 8. Further Research

In order to have further research more development needs to be conducted to ensure the reliability of the piezoelectric PVDF fiber after a conventional textile process such as in-lined poling and coating. Of course there are many suggestions for further research within this area other than optimization and some of these are listed below.

- Develop a prototype which can be used as a commercial product.
- Develop the bridge to conventional electronics: a connection between the fiber and the data recorder.
- Develop a visual projection of the recorded data in real time, giving a comprehensive image to all users.
- Characterize the time dependency of the applied strain which can be incorporated in software when used as a commercial product.

## 9. Acknowledgement

I would like to thank all participants in this very inspiring study, for making it worthwhile and the things I've learned. A special thanks goes to my supervisor *Anja Lund* whom has guided me throughout this project with wisdom. I am also very thankful of all the help, encouragement and inspiration my two consulting surgeons *Per-Ola Park* and *Maria Bergström* have given me throughout the project.

But there are also some people whom I'd like to thank from *The Swedish School of Textiles*; the two technicians *Catrin Tammjärv* and *Maria Björklund* for all help and encouragement, *Emanuel Gunnarsson* whom have always encourage me during stressful times and the bachelors in textile engineering for the company and encouragement.

There is no words to describe the huge appreciation I have for my family and friends who have supported me throughout, no matter the mood or how tiring I've been.

Anna Vahlberg

## 10. References

- Ashruf, C. M. (2002). Thin flexible pressure sensors. *Sensor Review, Vol 22 (Issue 4)*, 322-327.
- Atkins, P., & Jones, L. (2010). *Chemical Principles - The Quest for Insight*. New York: W.H. Freeman and Company.
- Bergström, M., & Park, P.-O. (2014, 05 13). Briefing about the current measuring systems implications. (A. Vahlberg, Interviewer)
- Bloom, D. A., Clayman, R. V., & McDougal, E. (1999). Stents and related terms: a brief history. *Urology, Volume 54, Issue 4*, 767-771.
- Carpi, F., & De Rossi, D. (2005). Electroactive polymer-based devices for e-textiles in biomedicine. *Information Technology in Biomedicine IEEE Transactions on* , 295-318.
- Crospon Inc. (2014). *Crospon Inc.* Retrieved from [www.crospon.com](http://www.crospon.com): <http://www.crospon.com/EndoFLIPTechnology.htm>
- Dargaville, T. R., Celina, C. M., Elliott, M. J., Chaplya, P. M., Jones, G. D., Mowery, M. D., . . . Martin, W. J. (2005). *Characterization, Performance and Optimization*. Albuquerque, New Mexico: Sandia National Laboratories.
- Das-Gupta, D. K., & Doughty, K. (1978). Corona charging and the piezoelectric effect in polyvinylidene fluoride . *Journal of Applied Physics*, 4601-4603.
- Ellis, H., & Mahadevan, V. (2013). *Clinical Anatomy : Applied Anatomy for Students and Junior Doctors (13th Edition)*. Somerset: Wiley.
- Fulmer, S. (1998). PVDF products. *Metal Finishing*, 87.
- Govari, A., & Fenster, M. (1997). *Patent No. US6053873 A*. USA.
- Gupta, S. (2010). E-textiles evolve to perform health monitoring functions . *ATA Journal Vol 21 Issue 2*, 29-33.
- Harrison, J. S., & Ounaies, Z. (. (2014, 02 28). *Piezoelectric Polymers (Online)*. Retrieved from <http://www.cs.odu.edu/~mln/ltrs-pdfs/icase-2001-43.pdf>
- Hasegawa, R., Kobayashi, M., & Tadokoro, H. (1972). Molecular Conformation and Packing of Poly(vinylidene fluoride). Stability of Three Crystalline Forms and the Effect of High Pressure. *Polymer Journal*, 591-599.
- Hoffer, L. (2009). *Patent No. US20110054333 A1*. USA.
- Hottle, T. A., Bilec, M. M., & Landis, A. E. (2013). Sustainability assessments of bio-based polymers. *Polymer Degradation and Stability* 98, 1898-1907.

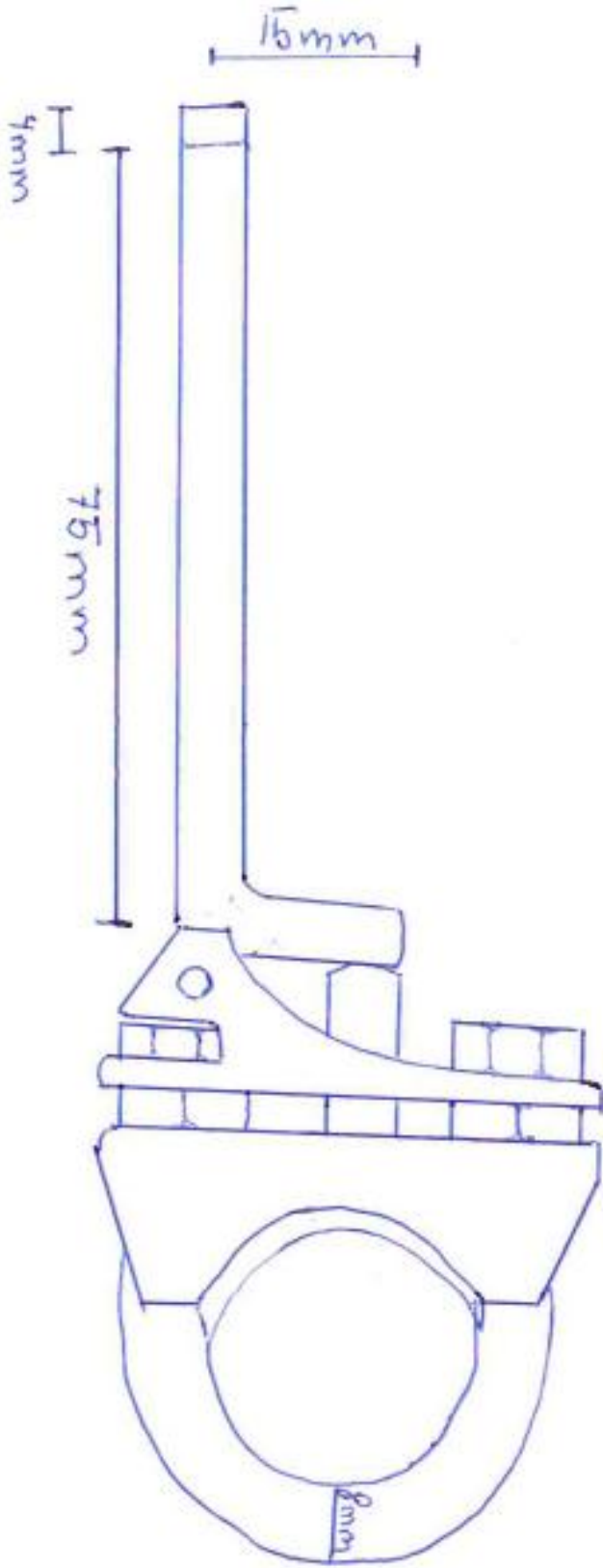
- Jezernik, S., & Grill, M. W. (2001). Optimal filtering of whole nerve signals. *Journal of Neuroscience Methods Vol 106 Issue 1*, 101-110.
- Kang, S.-G. (2010). Gastrointestinal Stent Update. *Gut and Liver, Vol 4*, 19-22.
- Kellow, J. E., Philips, B. S., Tucker, R. L., & Haddad, A. C. (1986). Human Interdigestive Motility: Variations in Patterns From Esophagus to Colon. *Gastroenterology*, 386-395.
- Liu, Z., Pan, C., Shen, Y., & Liang, P. (2013, March). Interfacial characteristics of polyethylene terephthalate-based piezoelectric multi-layer films. *Thin Solid Films*, 531, 284-293.
- Lund, A., & Hagström, B. (2010). Melt Spinning of Poly(vinylidene fluoride) Fibre and the Influence of Spinning Parameters on  $\beta$ -Phase Crystallinity. *Journal of Applied Polymer Science Vol. 16 (Issue 5)*, 2685-2693.
- Lund, A., Jonasson, C., Johansson, C., Haagensen, D., & Hagström, B. (2012). Piezoelectric polymeric bicomponent fibers produced by melt spinning. *Journal of Applied Polymer Science, Vol. 126 (Issue 2)*, 490-500.
- Mackay, C. D., Craig, W., Hussey, J. K., & Loudun, M. A. (2011). Self-expanding metallic stents for large bowel obstruction. *British Journal of Surgery*, 98(11), 1625-1629.
- Lando, J. B., & Doll, W. W. (1968). The polymorphism of poly(vinylidene fluoride). I. The effect of head-to-head structure. *Journal of Macromolecular Science, Part B: Physics*, 205-218.
- Matsushige, K., & Takemura, T. (1983). Crystal Transformation, Piezoelectricity, and Ferroelectric Polarization Reversal in Poly(Vinylidene Fluoride). *Polymer Science and Technology*, 115-137.
- Maudgil, D., Aviv, R., Williams, M., & Watkinson, A. (2001). Gastrointestinal stents - a review. *Radiography*, 153-158.
- Melgoza, E. L., Vallicrosa, G., Serenó, L., Ciurana, J., & Rodríguez, C. A. (2014). Rapid tooling using 3D printing system for manufacturing of customized tracheal stent. *Rapid Prototyping Journal*, 20(1), 2-12.
- Meng, H. (2009). Laser micro-processing of cardiovascular stent with fiber laser cutting system. *Optics & Laser Technology*, 41(3), 300-302.
- Murata, Y., Tsunashima, K., Umemura, J., & Koizumi, N. (1998, Feb). Ferroelectric properties of polyamides consisting of hepta- and nonamethylenediamines. *IEEE Transactions on Dielectrics and Electrical Insulation*, 5, 92-102.

- Nationalencyklopedin*. (2014). Retrieved 05 21, 2014, from www.ne.se:  
<http://www.ne.se/lang/anastomos>
- Nationalencyklopedin*. (2014). Retrieved 02 28, 2014, from www.ne.se:  
<http://www.ne.se/lang/tarm>
- Nationalencyklopedin*. (2014). Retrieved 2 28, 2014, from www.ne.se:  
<http://www.ne.se/lang/gastrointestinal>
- Nationalencyklopedin*. (2014). Retrieved 03 01, 2014, from www.ne.se:  
<http://www.ne.se/lang/saltsyra>
- Nationalencyklopedin. (2014, 03 02). *Nationalencyklopedin*. Retrieved from  
 www.ne.se: <http://www.ne.se/sfinkter>
- Nilsson, E., Lund, A., Jonasson, C., Johansson, C., & Hagström, B. (2013). Poling and characterization of piezoelectric polymer fibers for use in textile sensors. *Sensors and Actuators A: Physical Vol. 201*, 477-486.
- Noguchi, K. (1997, 11 01). System reliability of a sensor system considering the detectable area. *Electronics & communications in Japan. Part 3, Fundamental electronic science*, 80, 64-72.
- O'Brien, C. J. J., & Sparkman, S. R. (1997). What Is a Stent and Where Can You Get One? *The American Journal of Cardiology*, 79(9), 1306.
- Osman, R. M., Rahim Abd, M. K., Samsuri, N. A., Salim, H. A., & Ali, M. F. (2011). Embroidered fully textile wearable antenna for medical monitoring applications. *Progress In Electromagnetics Research Vol 117*, 321-337.
- PharmaCoDane, A. (2014, 05 13). *FASS*. Retrieved from www.fass.se:  
<http://www.fass.se/LIF/product?3&userType=2&nplId=19430311000013&docType=6>
- PicoTech. (2014, 03 01). *Pico Technology*. Retrieved from www.picotech.com:  
<http://www.picotech.com/oscilloscope.html>
- Qaiss, A., Saidi, H., Fassi-Fehri, O., & Bousmina, M. (2012, Dec). Cellular polypropylene-based piezoelectric films. *Polymer Engineering & Science*, 52, 2637-2644.
- Schwarz, A., Langenhove, L. V., Guermonprez, P., & Deguillemont, D. (2010). A roadmap on smart textiles. *Textile Process*, 99-180.
- Serwey, A. R., & Jewett, J. W. (2013). *Physics for Scientist and Engineers with Modern Physics 9th Edition/International Edition*. Gale: Brooks/Cole.

- Sirohi, J., & Chopra, I. (2000). Fundamental Understanding of Piezoelectric Strain Sensors. *Journal of Intelligent material Systems and Structures Vol 11 (Issue 4)*, 246-257.
- Thachuk, A. V. (2008). Stomach peptic ulcer: Confined gastric perforation. *Journal of diagnostic medical sonography, Vol 24*, 39-42.
- Tichý, J., Erhart, J., Kittinger, E., & Přívratská, J. (2010). *Fundamentals of Piezoelectric Sensorics*. Berlin: Springer-Verlag.
- Ward, K., Ounaies, Z., & Vetrovec, G. (2005). *Patent No. US 20090036975 A1*. USA.

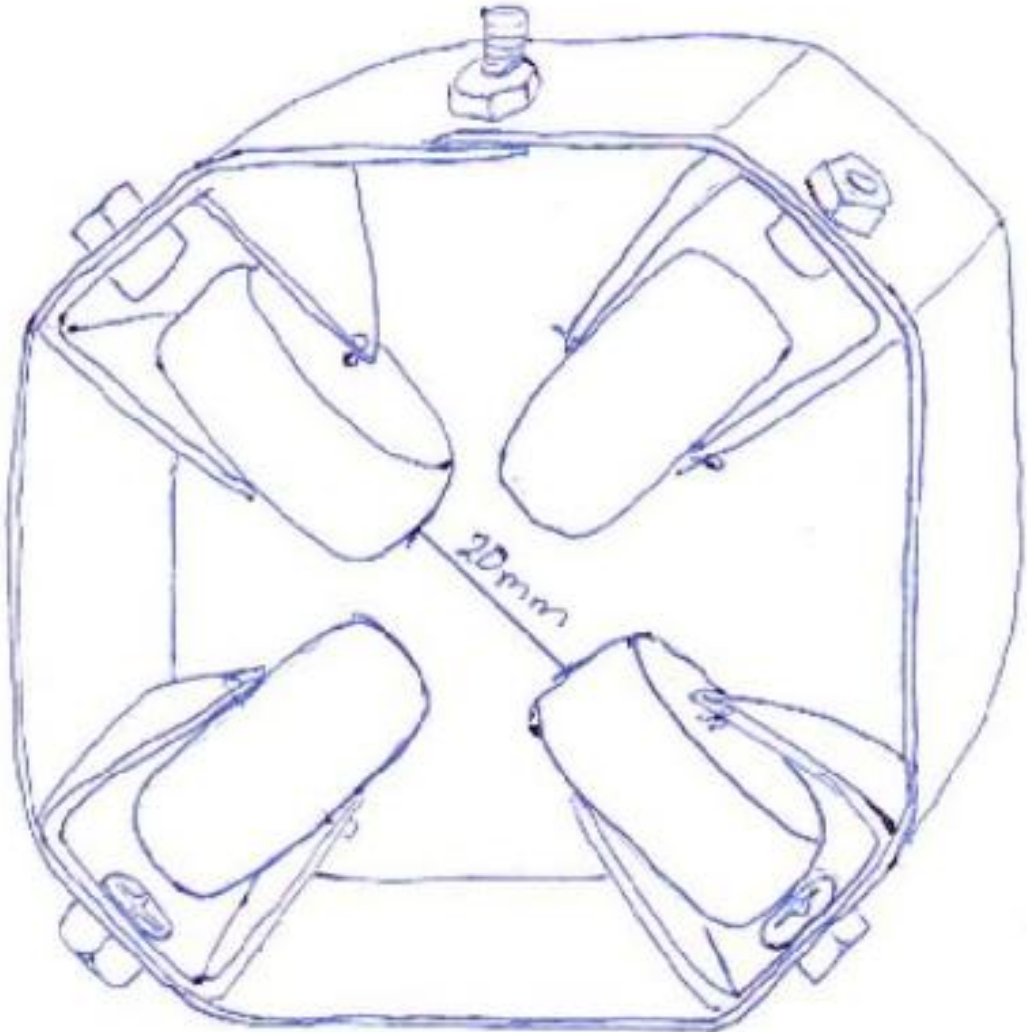
### Appendix A – Ring compression method

Below a display of the engineering drawings for the ring compression method is shown. The dimensions were measured with a Masuer caliper.



**Appendix B – Ring movement method**

Below a display of the engineering drawings for the ring compression method is shown. The dimensions were measured with a Masuer caliper.



### Appendix C – Sample 0

Settings for the PicoScope: a filtration of 10 Hz and a scale of 1 s/div. The x-axis is divided into seconds, where one square is one second. The y-axis is divided in mV where one square is 20 mV.

#### Hard surface

Test 2 is displayed below, where it is clear that the output for yarn A and B are higher than yarn C and D. The origin of the signal is from the corner where yarn A and B meet.

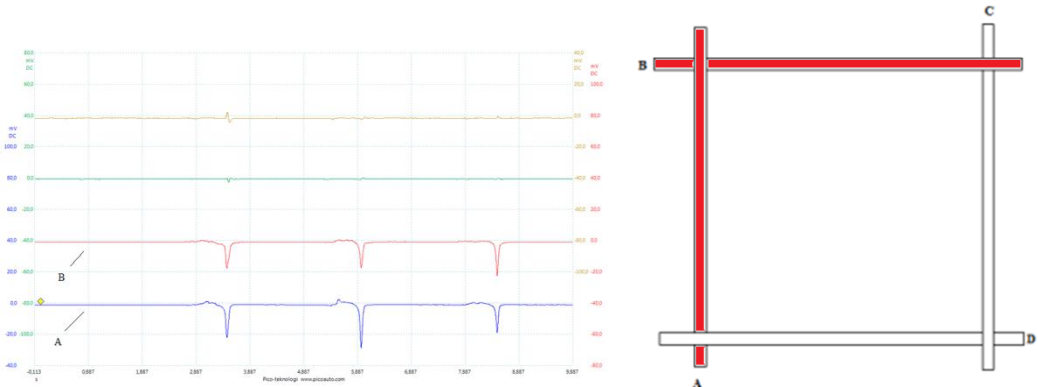


Figure 33 Testing in the corner of yarn A and B

Test 3 is displayed below, where it is clear that the output for yarn B and C re higher and gives the origin of the signal where yarn B and C meet.

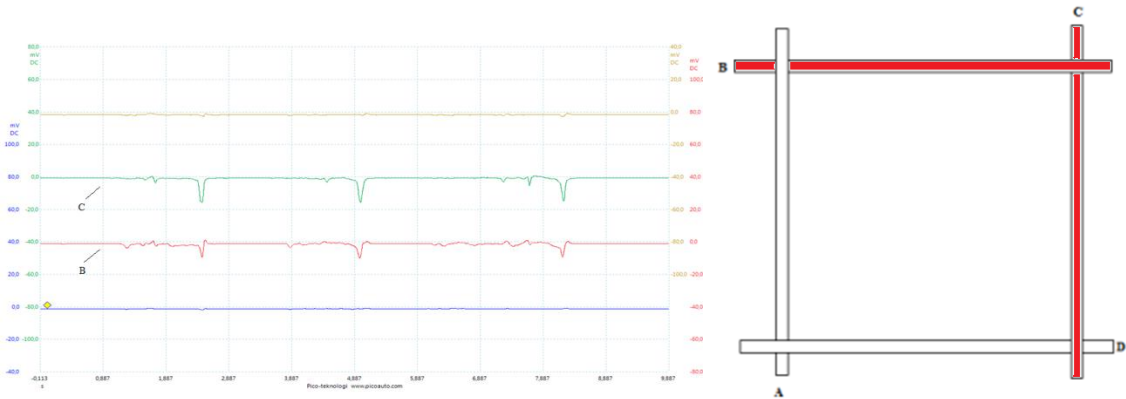


Figure 34 Testing in the corner of yarn B and C

Test 4 is displayed below, where it is clear that the output for yarn C and D, which gives the origin of the signal where yarn C and D meet.

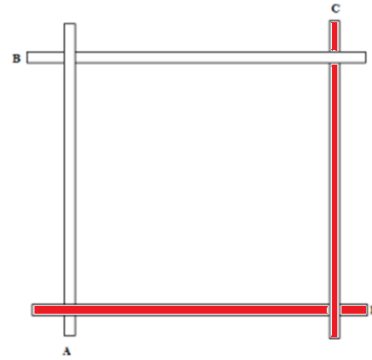
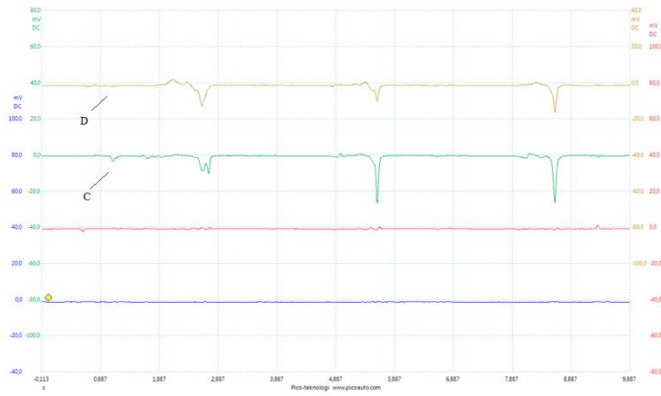


Figure 35 Testing in the corner of yarn C and D

### Elastic foam surface

Test 2 is displayed below, where it is clear that the output for yarn A and B are higher giving the origin of the signal where yarn A and B meet.

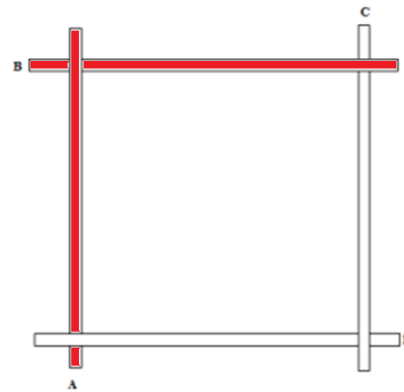
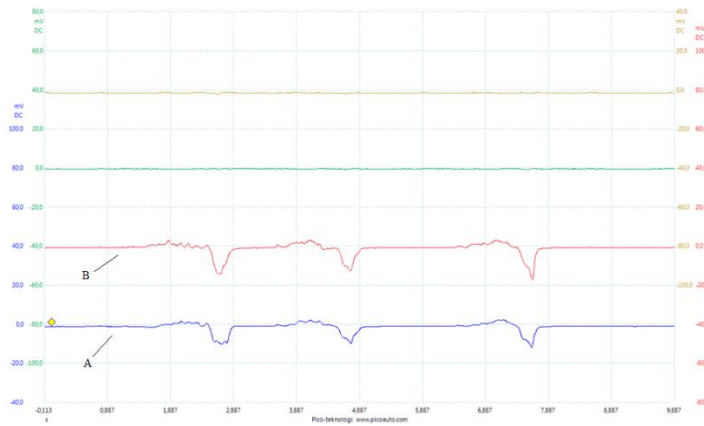


Figure 36 Testing in the corner of yarn A and B

Test 3 is displayed below, where it is clear that the output for yarn B and C are higher giving the origin of the signal in the corner where yarn B and C meet.

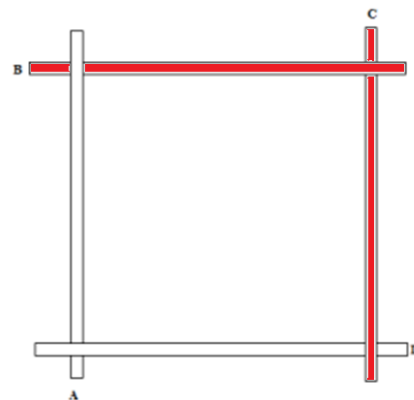
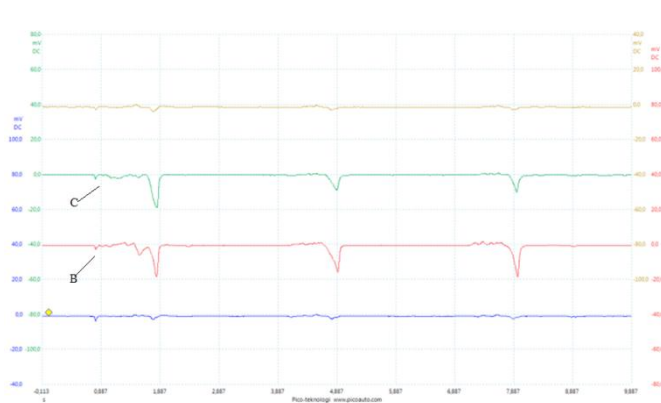


Figure 37 Testing in the corner of yarn B and C

Test 4 is displayed below, where it is clear that the output for yarn C and D are higher than the other yarns giving the origin of the signal in the corner where yarn C and D meet.

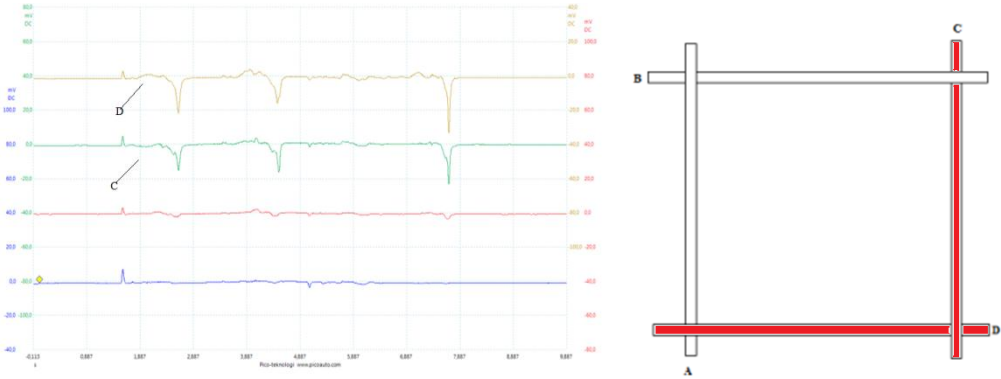


Figure 38 Testing in the corner of yarn C and D

# Appendix D – Curves ring compression method

Settings for the PicoScope: a filtration of 10 Hz and a scale of 1 s/div. The x-axis is divided into seconds, where one square is one second. The y-axis is divided in mV where one square is 20 mV.

## Sample 1

Test 2 is displayed below. Where the output is slightly larger for the vertical yarn E and F than for test 1, since the testing are is closer to yarn E and F.

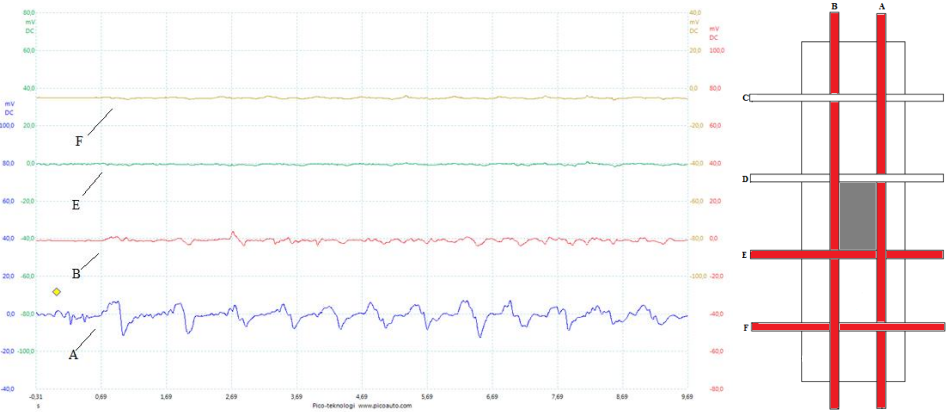


Figure 39 Where yarns A, B, E and F where tested in section 2

Test 3 is displayed below. Where the output is slightly larger for the vertical E and F than for test 2 due to the testing are is closer than test 1 and 2.

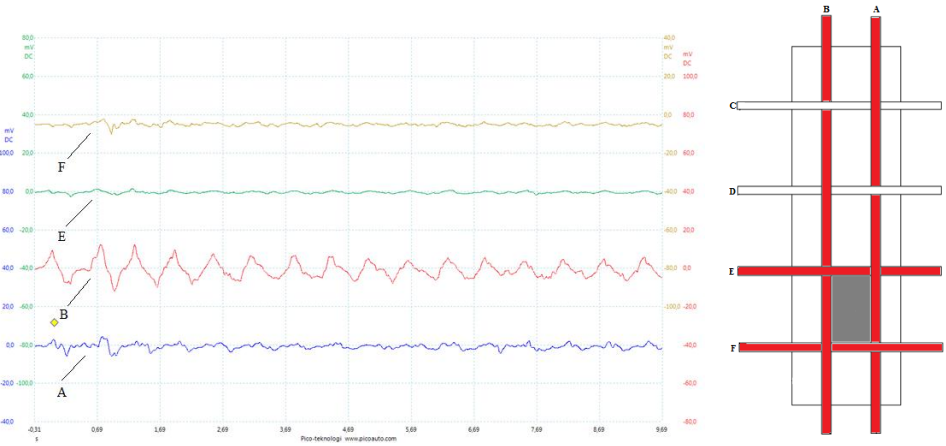


Figure 40 Where yarns A, B, E and F where tested in section 3.

Test 5 is shown in the figure below, where the output in the bottom curve is larger for the horizontal yarn A and a small output in the vertical yarns D, E and F.

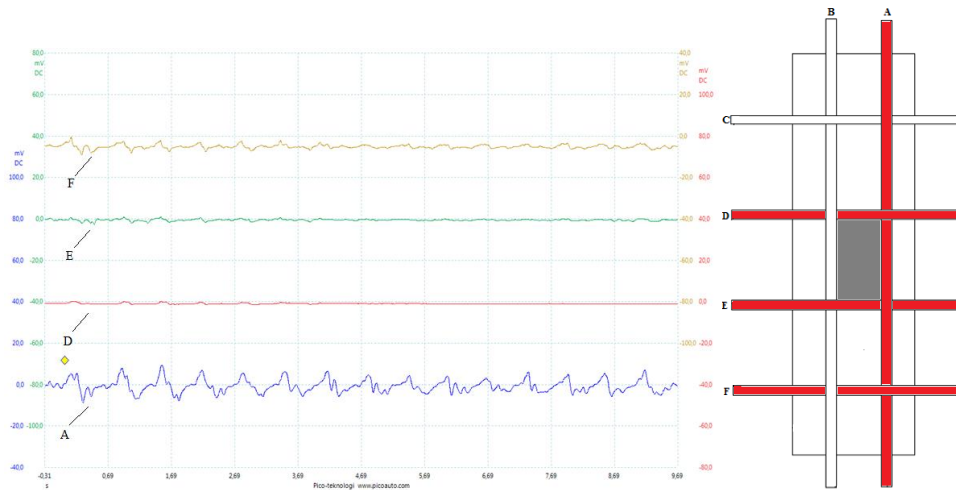


Figure 41 Where yarns A, D, E, and F and section 2 are tested.

Test 6 is displayed below. The output is large in the horizontal yarn as well as for the three vertical yarns.

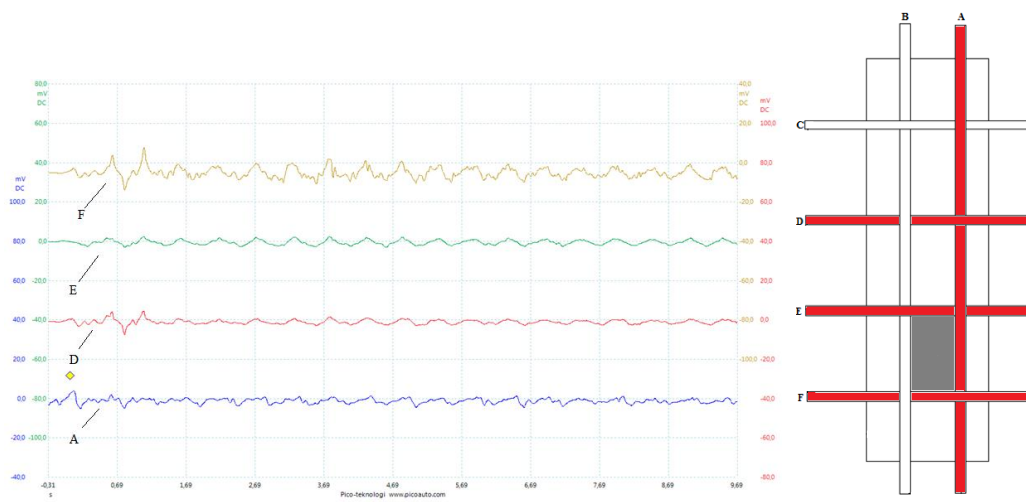


Figure 42 Where yarns A, D, E, and F and section 3 is tested

Test 8 is shown below in figure 47. Where the output signal is of the two bottom curves are higher than the two upper curves.

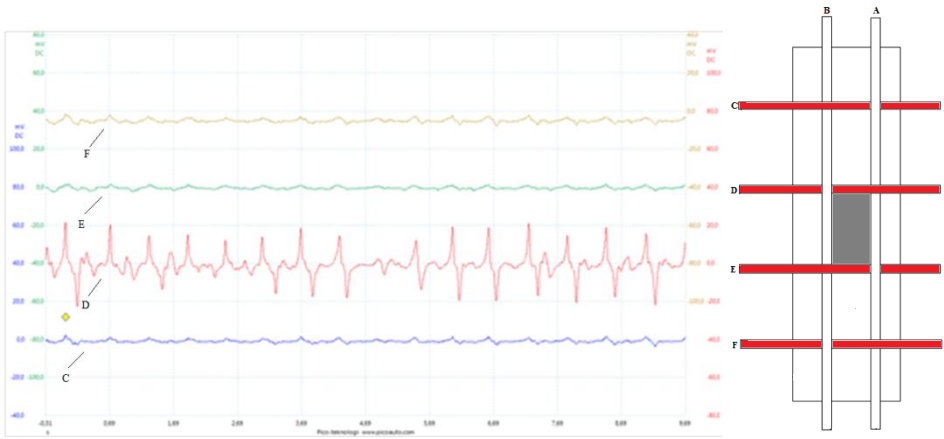


Figure 43 Where yarns C, D, E, and F and section 2 is tested

Test 9 is displayed in figure 48 below. Where the signals decrease from the top due to the testing area was section 3.

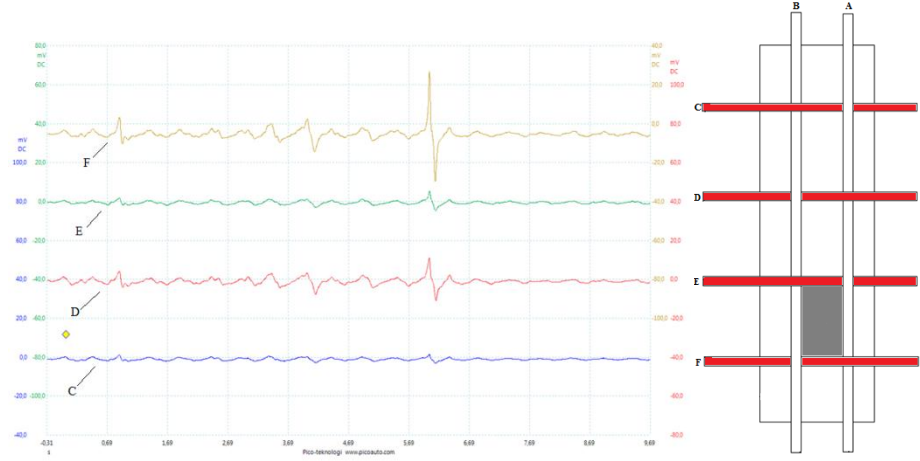


Figure 44 Where yarns C, D, E, and F and section 3 are tested.

Sample 2

Test 2 is displayed below in figure 49 where the output signals are higher for the horizontal

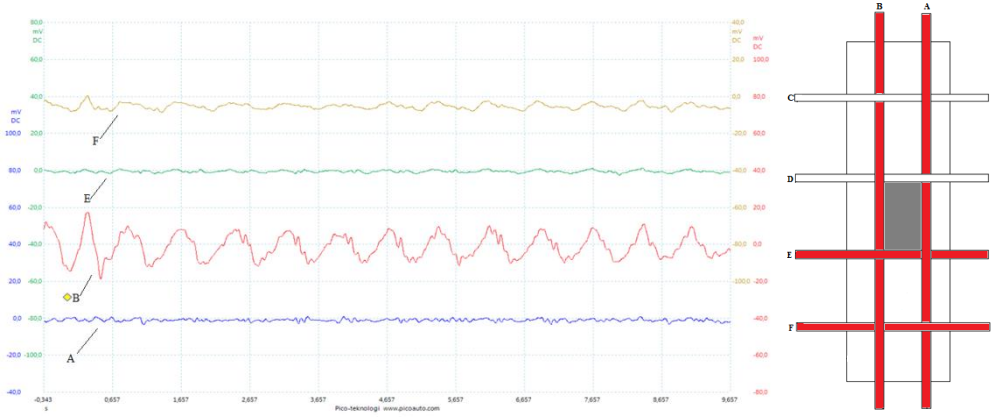


Figure 45 Where yarns A, B, E and F where tested in section 2

Test 3 is shown below, where the output signals for the horizontal yarn is higher than the vertical.

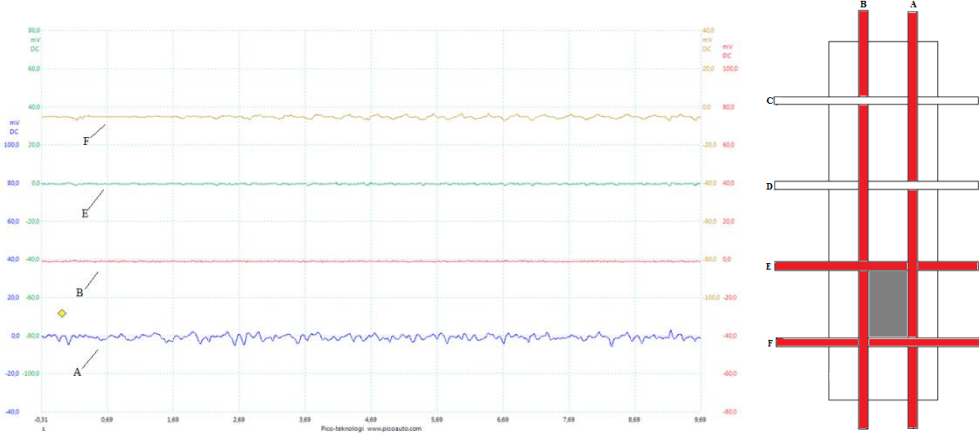


Figure 46 Where yarns A, B, E and F where tested in section 3.

Test 5 is displayed below in figure 51. Where there are output signals from the horizontal yarns as well as the vertical yarns.

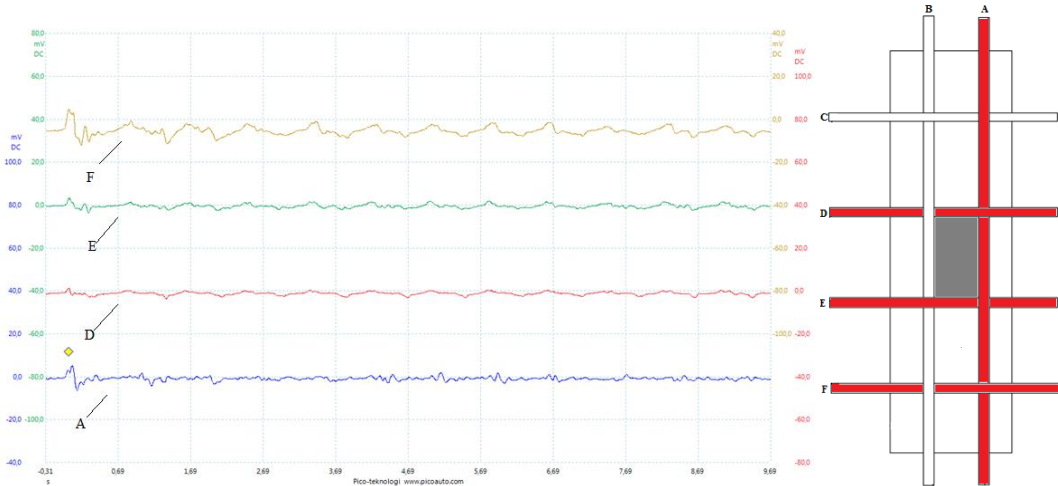


Figure 47 Where yarns A, D, E and F where tested in section 2.

Test 6 is shown in figure 52 below. Where there is output signal from the horizontal yarn and the vertical yarns.

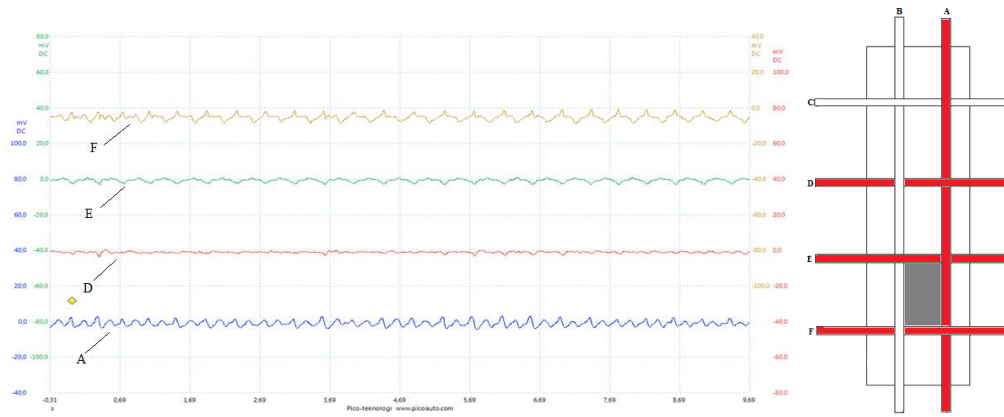


Figure 48 Where yarns A, D, E and F where tested in section 3.

Test 8 is displayed in the figure below, where the vertical yarns gives a high signal.

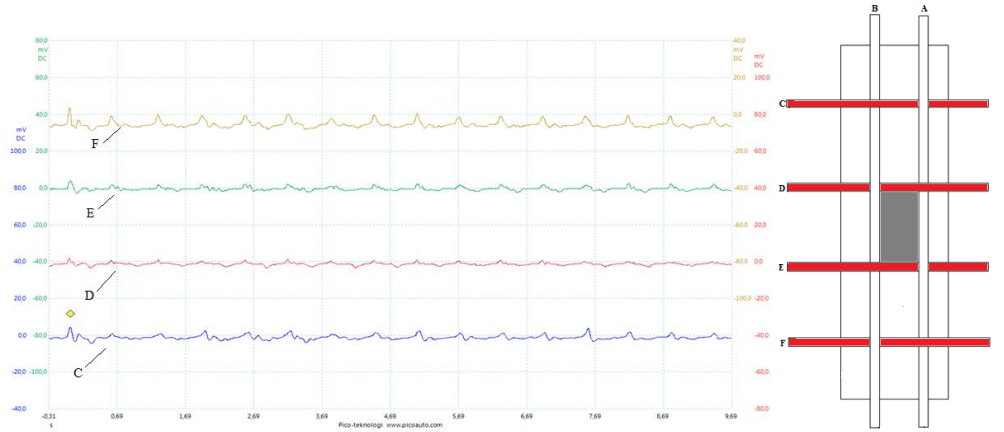


Figure 49 Where yarns C, D, E and F where tested in section 2.

Test 9 is displayed below in figure 54. Where the yarns E and F give and higher signal compared to C and D.

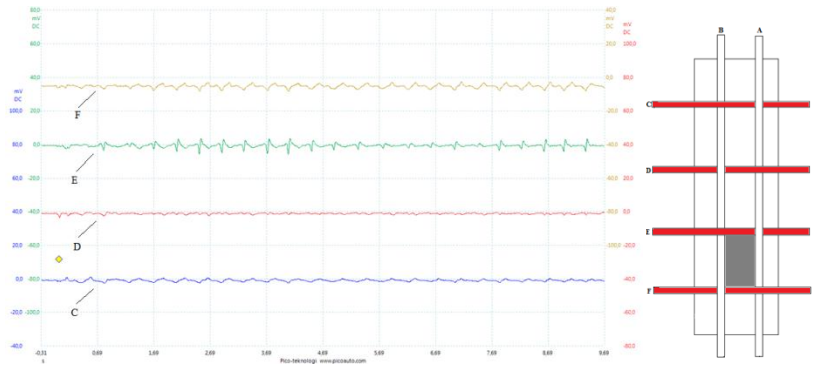


Figure 50 Where yarns C, D, E and F where tested in section 3.

## Double sided test

Test 2 is shown in figure X below where the yarns C and D is simultaneously tested in both sample 1 and 2. Where the first C and D from the bottom is sample 1 and the second C and D is sample 2.

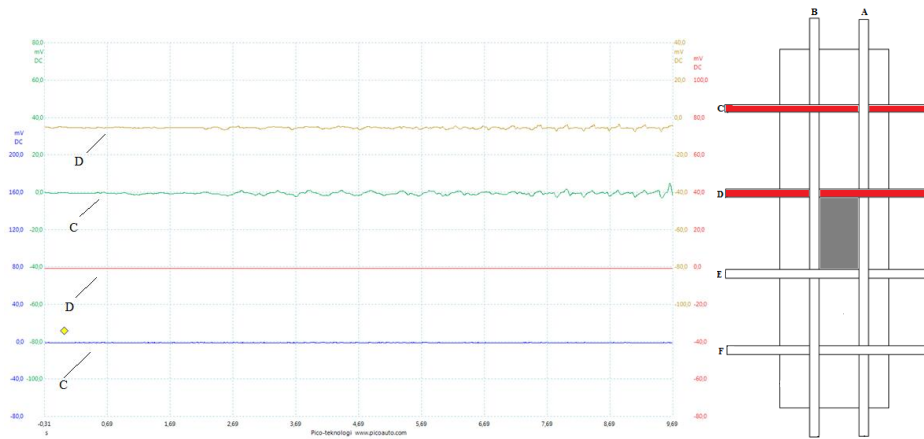


Figure 51 Where yarns C and D are tested in both sample 1 and 2 in section 2.

Test 3 is displayed below in figure 56, where yarns C and D are tested simultaneously in sample 1 and 2. Where the first C and D from the bottom is sample 1 and the second C and D is sample 2.

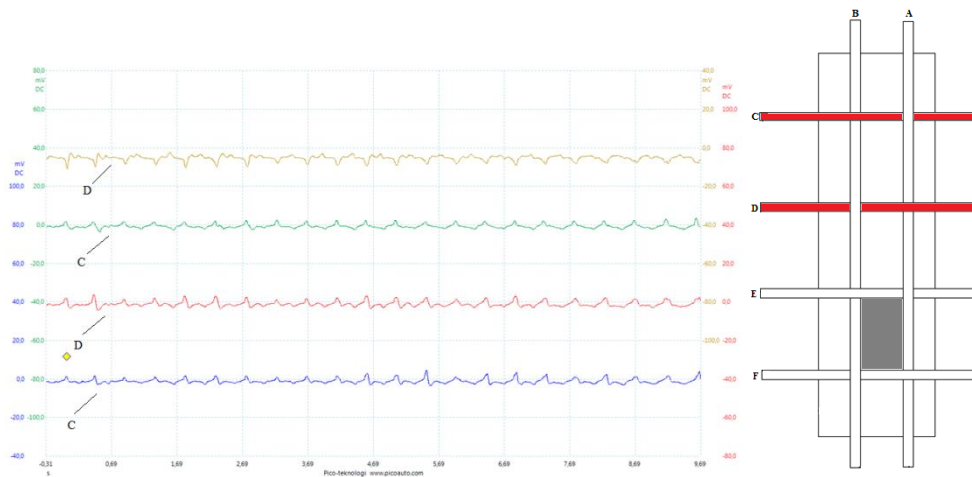


Figure 52 Where yarns C and D are tested in both sample 1 and 2 in section 3.

## Appendix E – Curves ring movement method

Settings for the PicoScope: a filtration of 10 Hz and a scale of 1 s/div. The x-axis is divided into seconds, where one square is one second. The y-axis is divided in mV where one square is 20 mV.

### Sample 1

The remaining two results are displayed here.

Test 2 is shown in figure X below, where the horizontal yarn A is the curve in the bottom and the three others is vertical placed yarns.

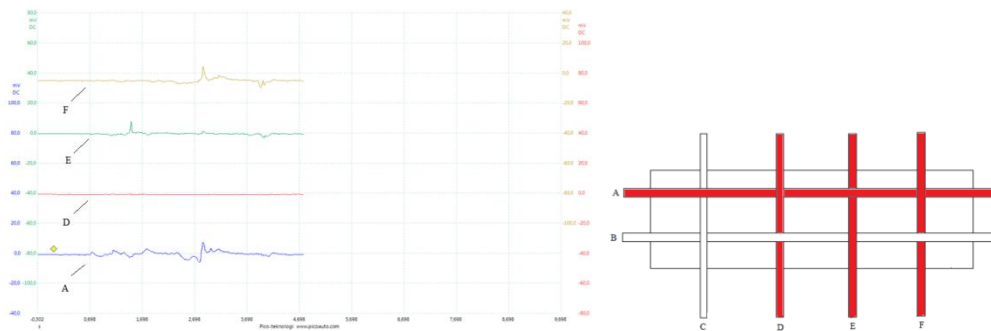


Figure 53 Where A, D, E, and F where the test started from the left side

Test 3 is displayed in figure X below, where all four vertically placed yarns.



Figure 54 Where C, D, E, and F where the test started from the left side

### Sample 2

The two remaining result are displayed here.

Test 2 is shown in figure X below. Where the bottom curve is the horizontal yarn A and the three upper curves had the same order from the bottom as follows D, E and F.

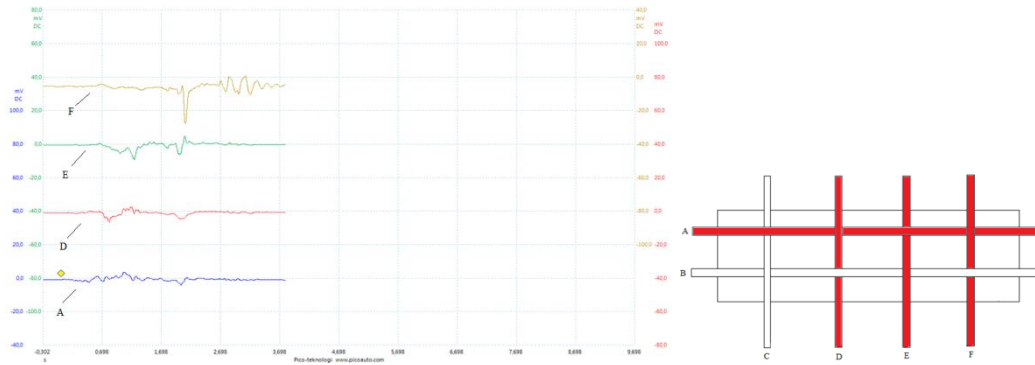


Figure 55 Where A, D, E, and F where the test started from the left side

Test 3 is displayed below where the curves have the same order from the bottom as for the tested vertically placed yarns: C, D, E and F.

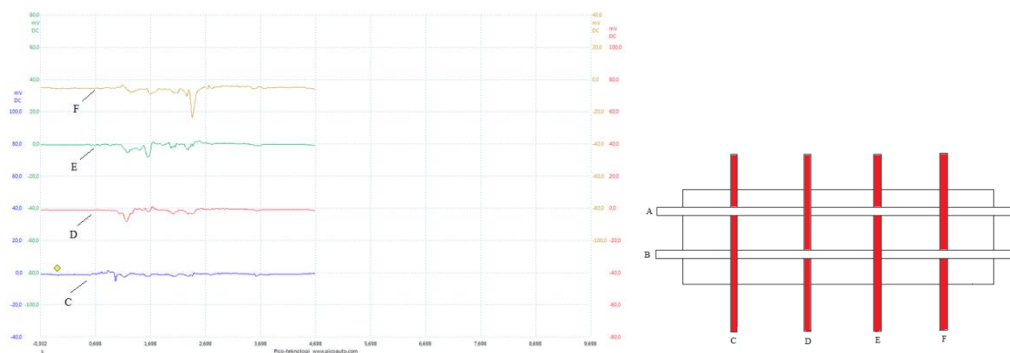


Figure 56 Where the yarns C, D, E and F were tested from the left side.

## Double sided test

The two remaining test result are displayed here.

Test 2 is shown in figure X below. Yarn C and D was tested in both structures simultaneously. Where the first C and D from the bottom is sample 1 and the second C and D is sample 2.



Figure 57 Where C and D were tested in sample 1 and 2 from the left side

Test 3 is displayed in figure X below. Yarn C and E was tested in both structures simultaneously. Where the first C and F from the bottom is sample 1 and the second C and F is sample 2.

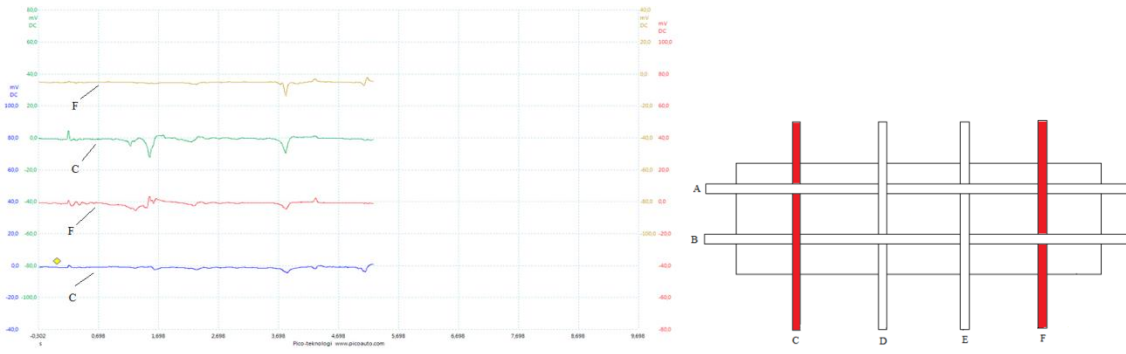


Figure 58 Where C and F were tested in sample 1 and 2 from the left side



THE SWEDISH SCHOOL  
OF TEXTILES  
UNIVERSITY OF BORÅS

Visiting address: Skaraborgsvägen 3 • Postal address: 506 30 BORÅS • Web: <http://www.hb.se/Textilhogskolan/>